

**Report On The Workshop On Models For Plasma Spectroscopy****St Johns College, Oxford****27th - 30th September 1993**

A meeting was held at St. Johns College, Oxford from Monday 27th to Thursday 30th of September 1993 to bring together a group of physicists working on computational modelling of plasma spectroscopy. The group came from the UK, France, Israel and the USA. The meeting was organised by myself, Dr Steven Rose of RAL and Dr. R W Lee of LLNL. It was funded by the US European Office of Aerospace Research and Development and by LLNL.

The meeting grew out of a wish by a group of core participants:

Dr R W Lee of LLNL, USA,
Dr S J Rose of RAL, UK,
Dr J Salter of SGCS Ltd, UK,
Dr W Goldstein of LLNL, USA,
Dr J Larsen of Cascade Applied Sciences Inc., USA,
Dr W Morgan of Kinema Research, USA,
Dr R Stamm of Universite de Provence, France,
Dr B Talin of Universite de Provence, France,
Dr A Calisti of Universite de Provence, France,
Dr A Bar-Shalom of NRCN, Israel,
Dr J Oreg of NRCN, Israel,

DTIC
ELECTE
S F D
MAR 03 1994

to make available to practising plasma physicists (particularly those engaged in the design and analysis of experiments) sophisticated numerical models of plasma physics. Additional plasma physicists attended the meeting in Oxford by invitation. These were experimentalists and users of plasma physics simulation codes whose input to the meeting was to advise the core group as to what was really needed!

Dr J Wark of Oxford University, UK,
Dr A Zigler of Hebrew University of Jerusalem, Israel and ARCO Inc., USA,
Dr A Djaoui of RAL, UK,
Dr J K Nash of LLNL, USA.

The meeting in Oxford follows an initial meeting of the group at Aix-en-Provence, France in 1991. The purpose of the meeting in Oxford was to review progress that the group had made and to lay down goals for further work. The method of distribution of the codes will be initially by means of a series of published books. Each book will cover a particular code or group of codes and the source will be available on disk together with the book. (Whilst the full source will generally be available, a stripped down version will be available from those participants (Drs Larsen and Morgan) whose companies already sell the full source as a product).

Although just publishing these books would be very useful to the community, what marks this project out as being significantly different to what has been done before is the development of a "Shell". This is a general piece of coding which sits above each

This document has been approved
for public release and sale; its
distribution is unlimited.

94 3 02 03 1

978 94-06860



of the individual codes. It allows a user to run any of the codes below it and to take the output for one code (perhaps a hydrodynamics simulation) and easily use it as the input for another code (perhaps one of the simple kinetic models). The Shell also allows easy graphing of results. In this way the Shell integrates the diverse codes - the whole suite operated under the Shell is more powerful than the sum of its parts. A brief description of each code is now given.

Shell

The SHELL has been developed by Dr Salter, of SGCS Ltd., UK. It has its own language which allows the user to take output from one code which can then be fed to another code.

A beta test version of the SHELL is complete and has been used at LLNL to write an atomic physics model-maker (a system which allows atomic physics data from diverse sources to be amalgamated to provide a comprehensive set of energy levels, collisional and radiative rates for a particular plasma). The write-up has been started but is not yet complete

Line-Broadening Code

The line-broadening code (called PIM PAM POM) has been developed by Drs Stamm, Talin and Calisti of the Universite de Provence, France. The code allows line shapes to be calculated for partially ionised ions including Doppler, lifetime broadening and Stark broadening (including both static and dynamic effects). Unlike previously well used line-shape calculations (e.g. R. W. Lee, JQSRT, 40, 561, 1988) which only consider H-like, He-like and Li-like ions, PIM PAM POM suffers no such restrictions and in principle can calculate line-shapes for transitions of open K-, L-, M- ...shell ions, although the size of the program in practice will restrict the number of levels being considered to at most one hundred. Such lines from ions of complex structure are now typically of interest in laser-produced plasmas, both as diagnostic of the plasma condition and also for fundamental line transport studies. The code reads in energies for the levels considered and the dipole matrix-elements between them. This is supplied by a separate detailed atomic physics calculation. With this information fully Stark-broadening line profiles are calculated for all the transitions between the levels specified.

PIM PAM POM is now complete and the write-up is almost complete.

Simple Models

Two models, FLY developed by Dr Lee of LLNL, USA and NIMP developed by Dr Rose of RAL, UK are simple kinetic models. FLY has been designed to provide a relatively detailed description of the time-evolution of the populations of H-like, He-like and Li-like ions in a plasma. Processes included are electron collision excitation and ionisation and their inverses as well as radiative recombination, spontaneous radiative de-excitation and dielectronic recombination. A time-varying (in general a non-Planckian) radiation field can also be supplied in which case the processes of photoexcitation and photoionisation and their inverses are also included. FLY can also

<input checked="" type="checkbox"/>	
<input type="checkbox"/>	
<input type="checkbox"/>	
<i>per lti</i>	
Codes	
id / or cial	

A-1

be coupled to spectral simulation codes which calculate the emitted spectra from the populations.

Whilst FLY allows calculations of the kinetics of open K-shell ions, NIMP allows calculations to be performed on open K-, L-, M-.....shell ions. This is possible by using a model which is less detailed. The average-atom model employed in NIMP follows the time-evolution of the plasma-averaged populations of the principal quantum shells. The population of specific states are then calculated from the shell populations using a simple combinatorial approximation.

Both FLY and NIMP are now complete and the write-up for each is also almost complete.

Detailed Atomic Physics Codes

Dr Bar-Shalom and Dr Oreg of NCRN, Israel and Dr Goldstein of LLNL, USA have developed a complex code called HULLAC to calculate accurate atomic properties of highly charged ions. The model has the same accuracy as the Dirac-Fock method, although for speed it is based on the parametric potential model. The user chooses a specific set of levels and the code then calculates accurate energies and oscillator strengths. Electron collisional excitation cross-sections are also calculated. A model to calculate electron collisional ionisation cross-sections is under development. Information from this code can be used, for example, as input data to the line-broadening code. Having produced accurate energy levels, collisional and radiative cross-sections the data can also be used in a simple matrix inversion steady-state population solver. This is currently under development.

Some developments of HULLAC need to be completed; the write-up is almost complete.

Hydrodynamics Code

Dr Larsen of Cascade Applied Sciences, USA has developed a one-dimensional Lagrangian hydrodynamics code, HYADES, with the main aim of simulating laser-plasma experiments, although it can be used to model other plasma sources. It includes models of laser absorption and thermal and radiation transport (either single or multigroup diffusion). The hydrodynamics follows shock wave propagation using a realistic material equation of state and the plasma is allowed to exhibit different free electron and ion temperatures, non-LTE ionic population and a non-Planckian radiation field. It can be used in planar, cylindrical or spherical geometry.

A stripped-down version of HYADES and the write-up are complete.

Non-Maxwellian Electron Distribution Code

The code ELENDF93 has been developed by Dr Morgan of Kinema Research, USA. It follows the time-evolution of the electron velocity distribution in a plasma and accounts for the effects of inelastic processes with ions and molecules (excitation and ionisation) which tend to force the distribution away from equilibrium and elastic collisions (between electrons) which tend to force the distribution back to a Maxwellian. Although the code was originally developed for low temperature, low density plasmas (in the lighting industry) it is felt that it will find application in high

density plasmas where similar effects are thought to occur, although very little work on non-Maxwellian electron distributions in these high density plasmas has yet occurred. A stripped-down version of ELENDF93 is complete as is the write-up.

Each of the above codes can interact under the SHELL. For example, an experimentalist wishing to analyse an X-ray laser experiment may firstly run the hydrodynamic code to ensure the laser/target combination results in a plasma which is sufficiently hot that the appropriate ions will be produced in the plasma. To analyse the X-ray lasing the atomic physics code will supply detailed energy levels for the ions concerned as well as rates from which the population can be calculated. Amplification depends critically on the line profile and this could be supplied by the line broadening code which would already have received all data files calculated for the atomic physics codes.

It is the integration of these codes that is their strength. The meeting in Oxford showed that great progress towards this aim had been made.

There follows copies of the transparencies of some of the talks presented at Oxford.

J. SALTER

SHELL TALK

ADAM -
A
DATABASE
ACCESS
AND
MANIPULATION
LANGUAGE

OUTLINE OF PRESENTATION

- . AIMS
- . ARCHITECTURE OF ADAM
- . ADAM FEATURES
- . FUTURE WORK

AIMS

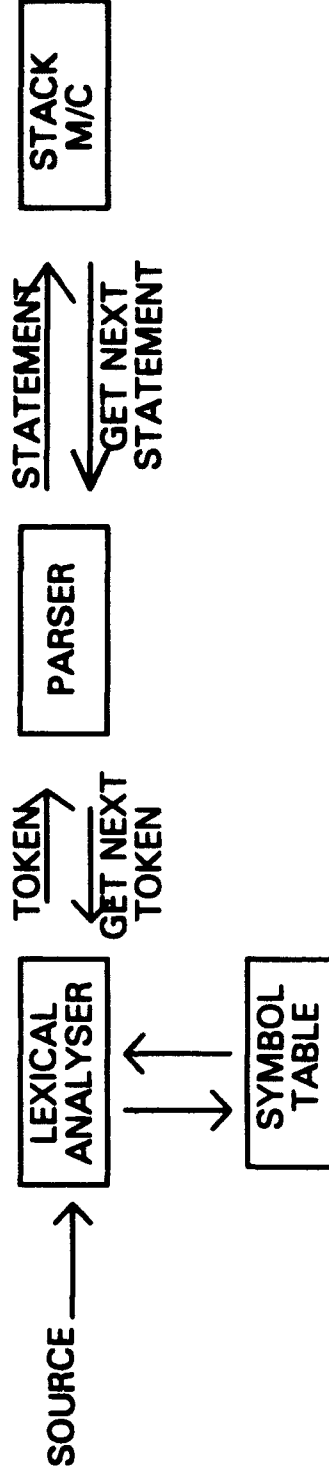
- **User Centred Development**
 - to provide a mechanism to allow users to solve their problems and not be constrained by the need to learn about the environment or limited by the processing capability offered by their environment
- **For model making, need :**
 - access to database to retrieve data
 - manipulation of data
 - graphical representation of results

AIMS

- **Portable Development**
 - develop in UNIX environment
 - use standard UNIX tools
 - isolate ADAM from specific products by using abstract interfaces for portability
 - for database, abstract interface based on SQL
 - for plotting, abstract interface based on GKS (X Windows)
 - for interprocess communications, abstract interface based on BSD sockets

ARCHITECTURE

- ADAM interpretive for ease of use
- each statement parsed and executed to allow rapid prototyping approach



ARCHITECTURE

- **Lexical Analyser:-**
 - reads input stream and identifies tokens (on the basis of white space and non-alphabetic characters in ADAM)
- **Parser:-**
 - parses sequence of tokens, recognises statements and generates internal code for Stack Machine (= YACC in ADAM)
- **Stack Machine :**
 - reads internal code and executes
- **Symbol Table**
 - Stores symbols for later reference :- name, type, data (for simple elements)

ARCHITECTURE

- For example, take the statement :

$$x = y + 1$$

(assume x and y are INTEGER)

- Lexical Analyser produces :-

TOKEN	ATTRIBUTE
INTEGER	x
EQ	
INTEGER	y
ARITHOP	+
NUMBER	1

ARCHITECTURE

. Assume definition of language includes :-

STMT : EXPR EQ ARITHOP

EXPR : INTEGER

 | NUMBER

EQ : '='

ARITHOP : EXPR '+' EXPR

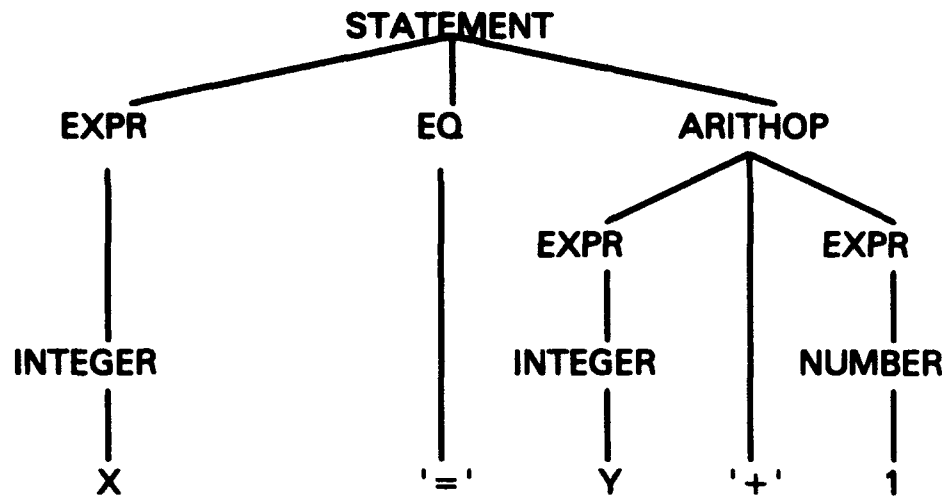
 | EXPR '-' EXPR

 | EXPR '*' EXPR

 | EXPR '/' EXPR

parser produces a parse tree :-

ARCHITECTURE



ARCHITECTURE

- Internal representation produced by syntax directed translation using a stack
- Using the definition of language from earlier :-

STMT : EXPR EQ ARITHOP {EXECUTE}

EXPR : INTEGER {PUSH \$1}

| NUMBER {PUSH \$1}

EQ : '=' {CODE ASSIGN}

ARITHOP : EXPR '+' EXPR {CODE ADD}

| EXPR '-' EXPR {CODE SUB}

| EXPR '*' EXPR {CODE MULT}

| EXPR '/' EXPR {CODE DIV}

ARCHITECTURE

EXECUTE	execute code
ASSIGN	pop 1 element and assign
ADD	pop 2 elements, add and push result onto stack
DATA STACK	CODE FIFO
NUMBER (1)	ADD
INTEGER (Y)	ASSIGN
INTEGER (X)	

Cf. Postfix 1 $y + x =$

- stack machine reads instructions from Code FIFO and executes in sequence

ARCHITECTURE

- **YACC based on LALR method which has several advantages :**
 - **can handle virtually any language construct including simple statements and complex expressions**
 - **traps syntax errors as early as possible**

ARCHITECTURE

- Object oriented design for portability
 - opaque data types with well defined interfaces, e.g. database, structures
- layered design
 - user interface
 - input from keyboard or script files
 - text or graphical output
 - processing
 - database
- error trapping provides user assistance via meaningful messages
 - e.g., syntax checking on input, type checking on all statements and expressions

ADAM LANGUAGE FEATURES

- language format
- strongly typed
- rich vocabulary
- database access
- graphical output
- user defined extensions

LANGUAGE FORMAT

- **ADAM language consists of a series of statements**
- **similar to C in versatility and features but with enhancements for naive users including :**
 - **integrated database access**
 - **integrated graphical output**

TYPING

- type checking means that operators have operands that are permitted by the language specification, e.g. it may be forbidden to use a real number to index an array
- type checking avoids many problems with inconsistent data type manipulation, e.g. function parameters
- ADAM supports strongly typed operators and expressions
- several types are supported :
 - INTEGER
 - DOUBLE
 - STRING
 - STRUCTURE (user defined records)
 - POINTERS FOR THE ABOVE
- ADAM also supports arrays of the above types

BASIC VOCABULARY

- **statements include :**
 - **expressions**
 - **numeric**
 - $(x+3)*y$
 - **string**
 - `strlen("hello world")`
 - **pointer**
 - `a = &b`
 - **+, -, *, /**
 - **BOOLEAN**
 - $(a \parallel b) \&\& (c \parallel d)$
 - **compound statement, { }**
 - **pointer arithmetic**
 - `&a + 3`

BASIC VOCABULARY

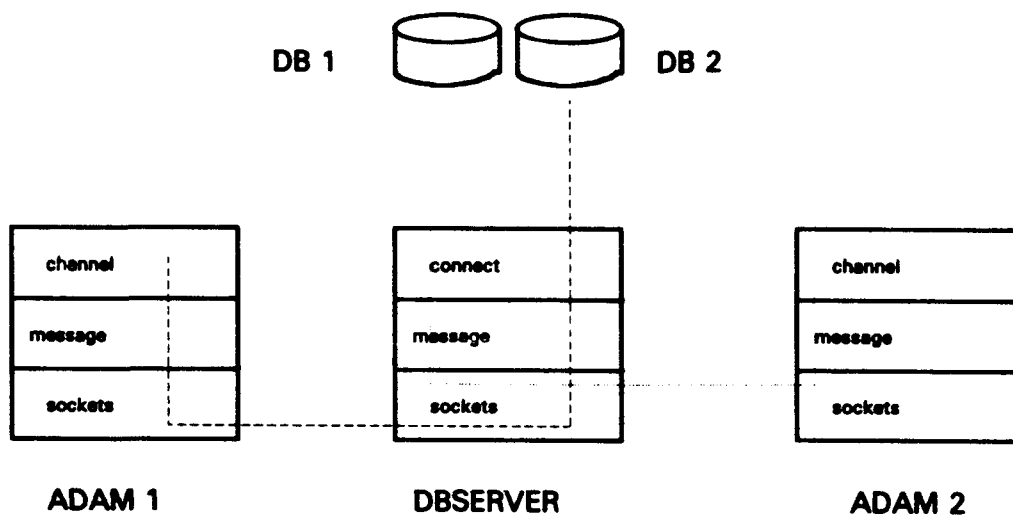
- control
 - if / else
 - if a then b else c
 - while
 - while a { ... }
 - for
 - for (i=1; i < 3; i = i + 1) { ... }
 - switch
 - switch a; case 1: ...

BASIC VOCABULARY

- **variable declaration**
 - **declare integer a, b, *c, *d(2:3, 4:5)**
- **include files**
 - **include file "/tmp/a"**
- **memory manipulation**
 - **a = malloc (3)**
- **string functions**
 - **a = strlen(b)**

DATABASE PROCESSING

- self configuring database access
 - the table schemas are accessed by ADAM and stored at connection time
- ADAM isolated from database by server process
 - allows several ADAM processes to access a database concurrently
 - allows one ADAM process to access several databases concurrently



- can read data of all atomic types supported by database

DATABASE PROCESSING

• sample code :

declare dbvar da

declare integer rows

/* open database adb1 */

dbopen adb1

/* access data */

rows = dbread adb_col1 as col1 into da from
adb1 where adb_col1 > i

if (rows > 0)

{ /* use data */

i = da:col1

}

/* close database */

dbclose adb1

GRAPHICAL OUTPUT

- can display graph using linear or logarithmic scales
- several graphs may be displayed at one time
- can add and remove graphs dynamically

GRAPHICAL OUTPUT

. sample code :

```
declare plotvar pv
```

```
declare plotelem pe1, pe2
```

```
declare integer ia1(10), ia2(10), index
```

```
      /* initialise arrays */
```

```
for (index = 1; index < 11; index = index + 1)
```

```
{
```

```
    ia1 (index) = 2 ^ index
```

```
    ia2 (index) = 3 ^ index
```

```
}
```

GRAPHICAL OUTPUT

/* create a new graph */

pv = newplot loglin

/* add a plot */

pe1 = addplot pv ia1

/* display the graph */

frame pv

/* add another plot and display*/

pe2 = addplot pv ia2

frame pv

/* remove a plot and display */

remplot pv pe1

frame pv

/* destroy the graph */

freeplot pv

USER DEFINED EXTENSIONS

- two types :
 - user definable functions and procedures written using ADAM
 - escape to C/FORTRAN to allow reuse of existing code
- both types are fully integrated with ADAM code
- type checking for parameters and return values in both cases
- local variable scoping in case 1

FUTURE

- **several ideas**
 - **allow database update**
 - **improve useability via GUI**
 - **modify command syntax in light of usage**
 - **either remove or document "undocumented features"**

Ultra Fast Line Shape Code for Plasma Spectroscopy

Annette Calisti
Roland Stamm
Bernard Talin

and

Dick Lee



Main purposes of this code:

- friendly, small and fast enough to run on workstations
- bridging the gap between the simplest hydrogen lines and the unresolved transition arrays
- accounting for stochastic Stark effect

Atomic physics for emitters

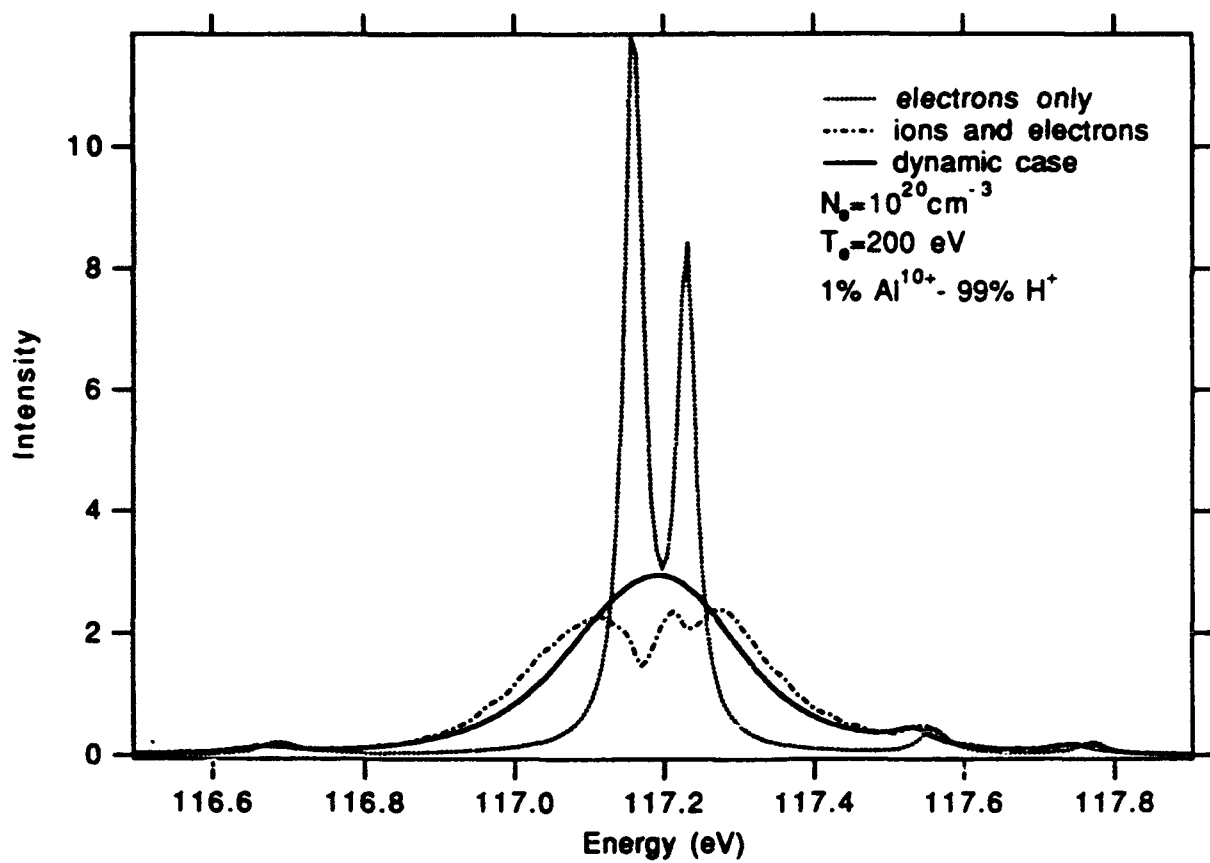
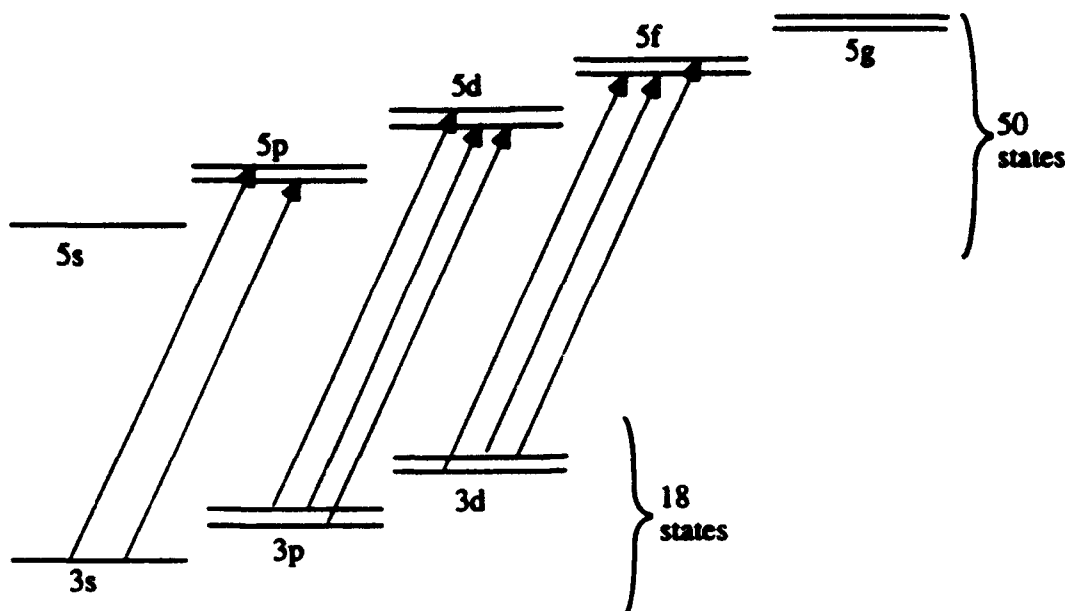
Plasma physics
non equilibrium level populations
ion microfield statistics

CODE
binary collisions with electrons
homogeneous broadening

coupling with ion microfields
stochastic Stark broadening

miscellaneous broadening (Doppler and apparatus)

line shape



Theoretical background

The radiated intensity is given by:

$$I(\omega) = \frac{1}{\pi} \Re \int_0^{\infty} e^{i\omega t} \langle \vec{d}^* | U(t) | p_0 \cdot \vec{d} \rangle dt$$

where $U(t)$ is solution of a Liouville stochastic equation

$$\begin{cases} \frac{dU_f(t)}{dt} = -i(L_0 + I_f)U_f(t) \\ U_f(0) = 1 \end{cases}$$

and

$$U(t) = \langle U_f(t) \rangle_f$$

$$\begin{cases} \frac{dU_f(t)}{dt} = -i(L_0 + I_f)U_f(t) \\ U_f(0) = 1 \end{cases} \quad \text{and} \quad U(t) = \langle U_f(t) \rangle_f$$

A numerical resolution of this equation could involve a huge data set $\text{rank}^2 \times N_{\text{step}} \times N_{\text{history}} \approx 10^{12}$

Such a complete simulation can be used for very small systems.

For MMM a special Markovian function space is used. An analytical solution exists for $U(t)$.

For a more general purpose an other method must be found.

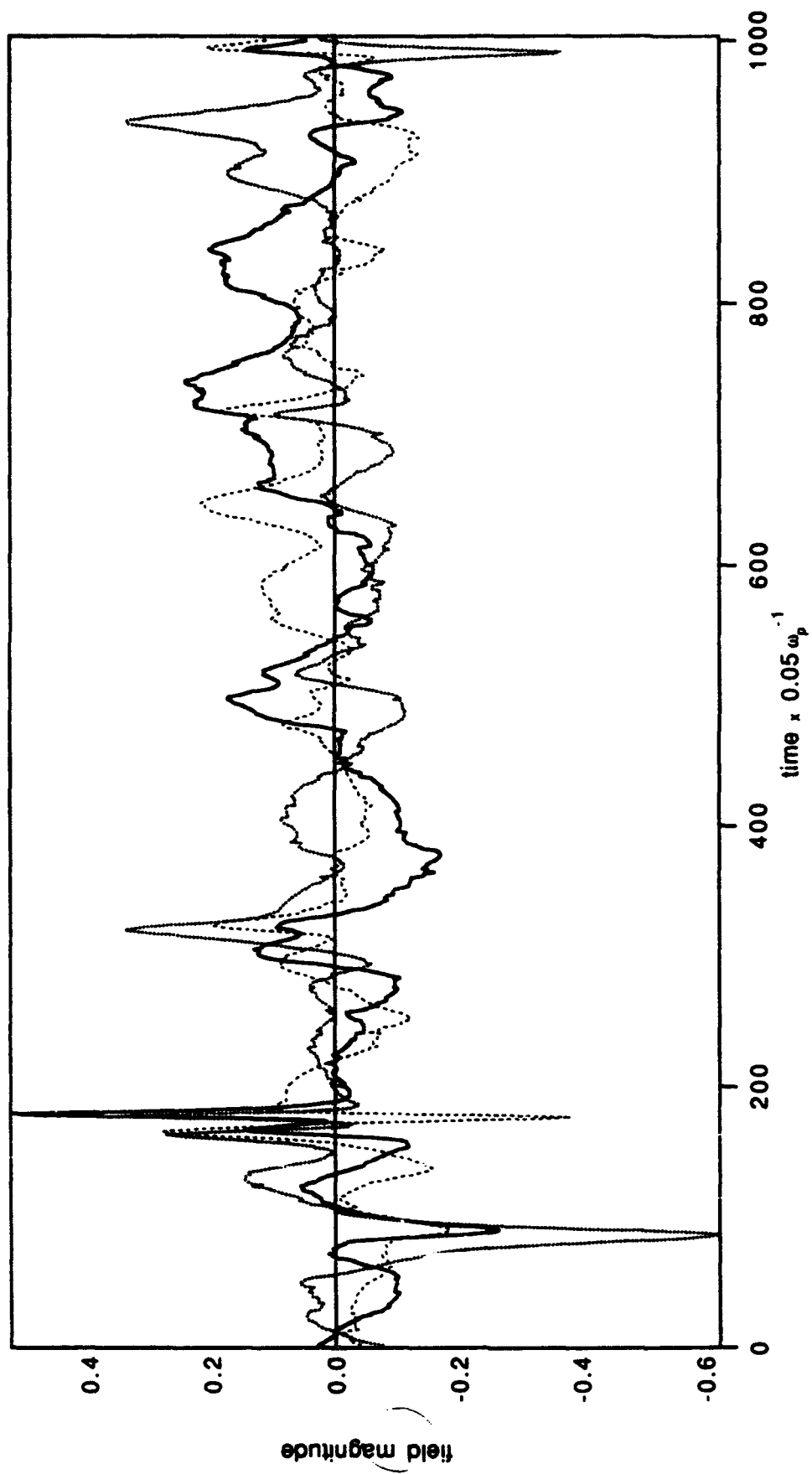
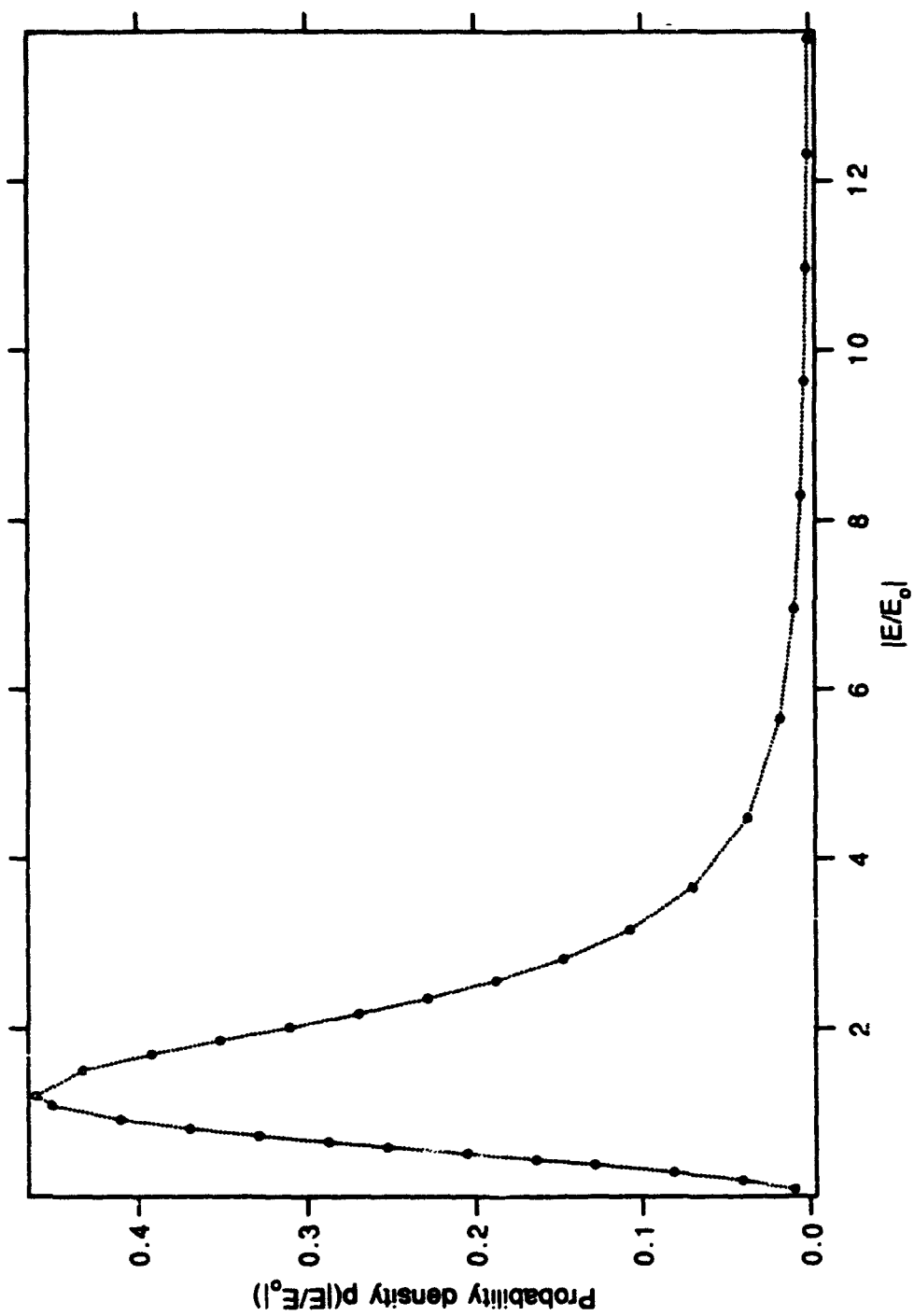
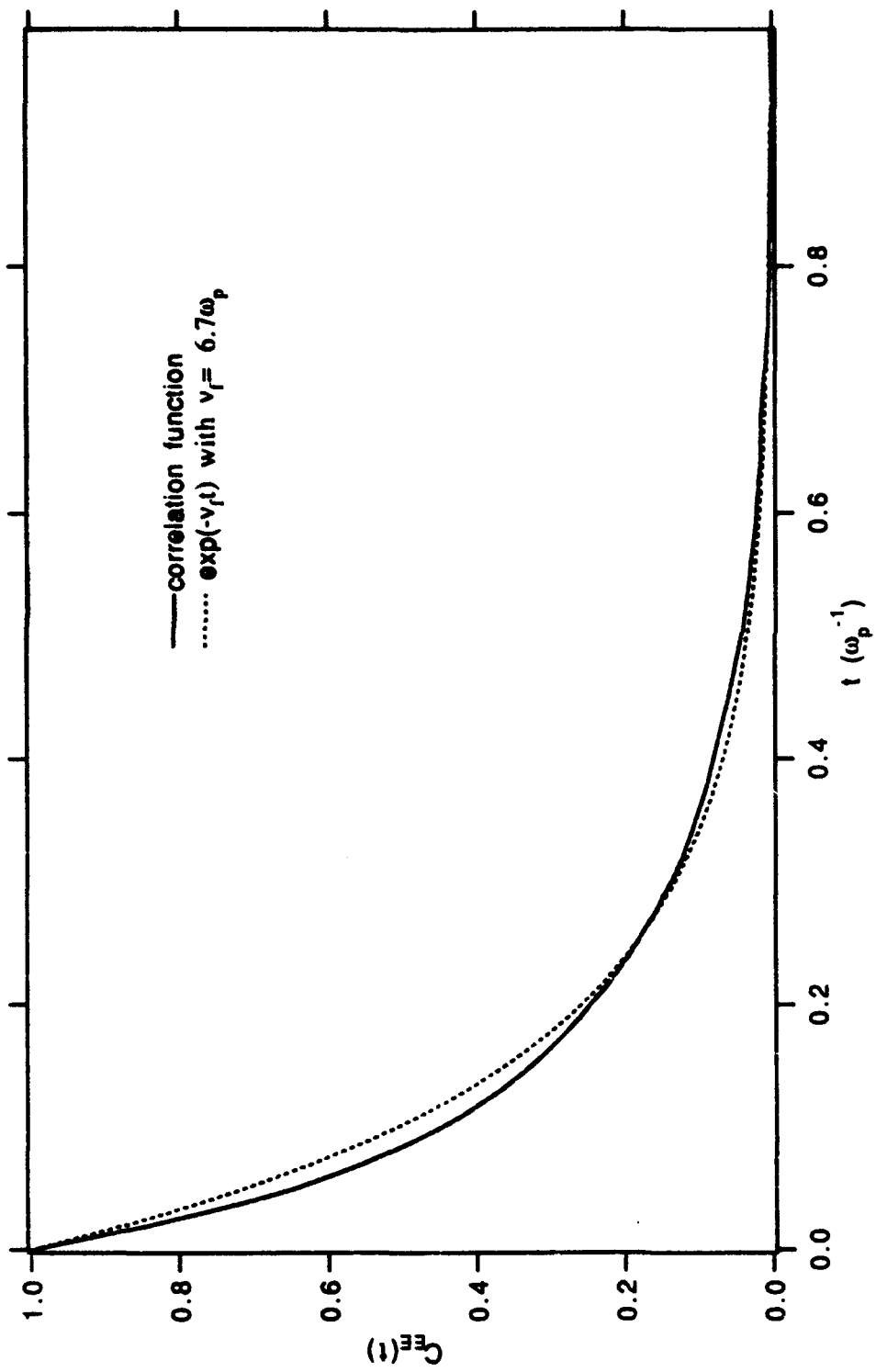


FIGURE 1



A_r^{17+}
 $N_e = 1.5 \cdot 10^{23} \text{ cm}^{-3}$
 $T_e = 860 \text{ eV}$

FIGURE 2



Ar^{17+} in proton plasma
 $N_e = 10^{24} \text{ cm}^{-3}$
 $T_e = 10^7 \text{ K}$

FIGURE 3

Frequency fluctuation model

1st hypothesis: as for MMM all the information needed to solve the SLE is involved in the static Stark components and in the field fluctuation rates.

2nd hypothesis: a coarse grained distribution of the Stark components exists and has the same stochastic behavior than the primitive set.

3rd hypothesis: the line shape results from a Markovian fluctuation of the above coarse radiative channels

$$I(\omega) = \Re \sum_{i,j} (\omega - f + iW + i\gamma)_{i,j}^{-1} (a_i + ic_i)$$

where

$$W_{i,j(i \neq j)} = \nu p_i, \quad W_{i,i} = -\nu(1 - p_i) \quad \text{with} \quad p_i \propto a_i$$

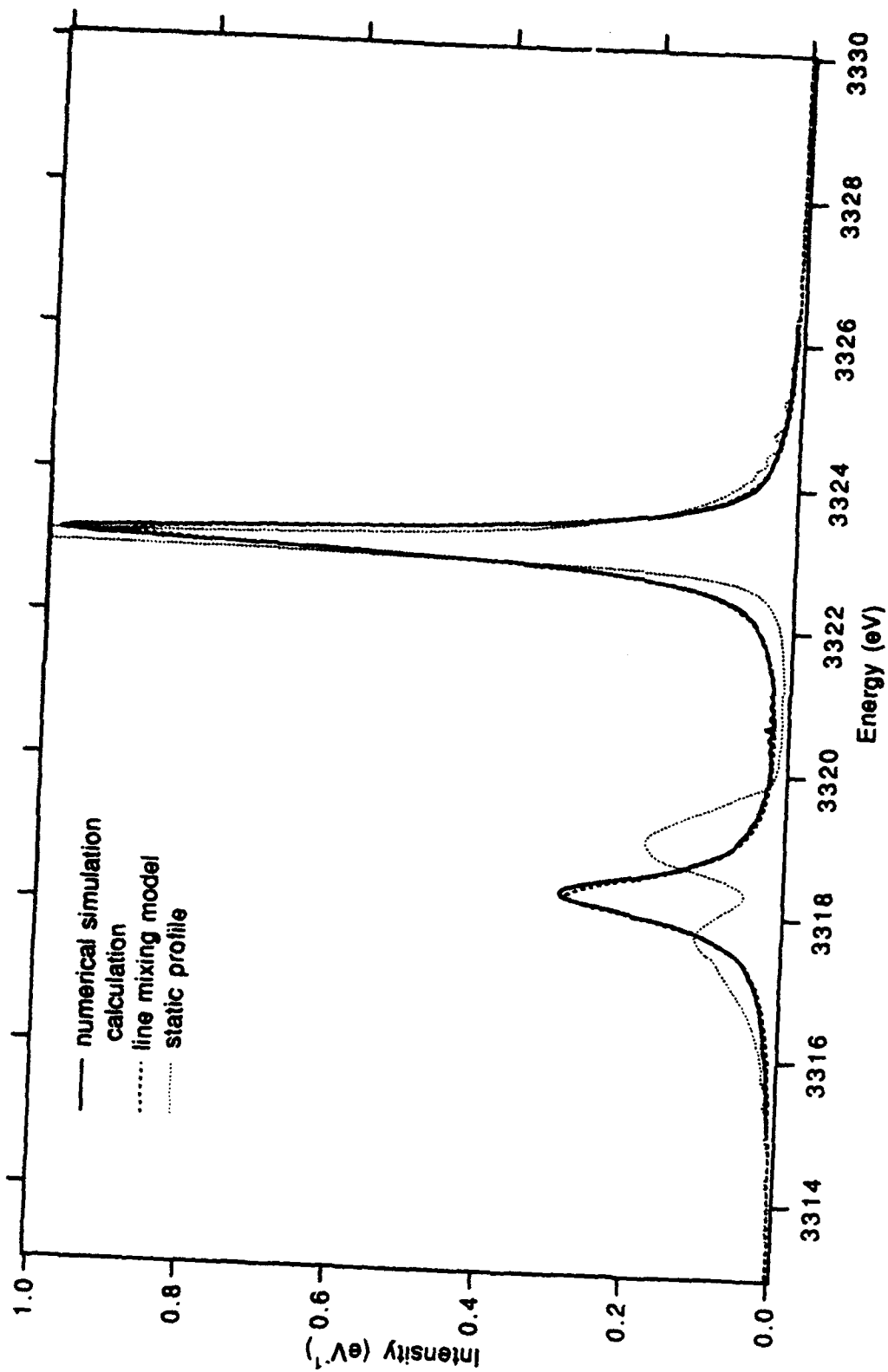


FIGURE 8

Code organization:

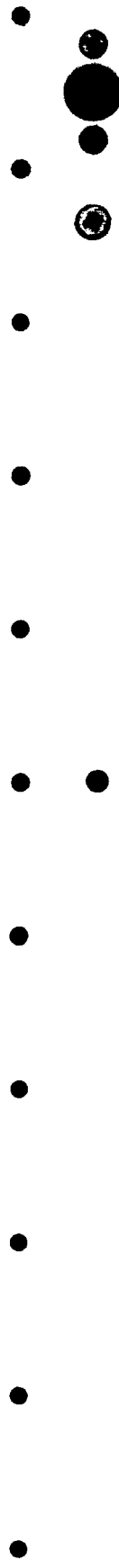
Four different phases are used:

0-customization

1-inputs and data preparation

2-calculation of the stochastic Stark components

3-line shape post-processing



```

bas.dat
***
outs.dat
outd.dat
c      s
40.00  1.00
17.    1.
0.1000E+08 0.1000E+08
0.1000E+25 0.1000E-01
3313.0    3326.0
50        2
2        10.
0.010     0.100
new data?

(base) name of the data base
(pof) name of the population file
(sout) output static file
(dout) output dynamic file
(roc,ydn) options: real:r cmplx:c stat:s dyn:d
(atomw,amp) emitter / perturber mass (a.u.)
(ze,zp) net emit. charge / pert. charge
(tmpe,tmpi) electron temp. / ion temp. (kelvin)
(dens,per) elec. dens. / emit./pert. percentage
(da,db) bounds of the frequency interval (eV)
(nmc,nu) m-fld number / block rad. trans. numb.
(lay,xset) layer number / stark trans. cutoff
(pxlo,pxhi) merging parameters low/high

```

Conclusion:

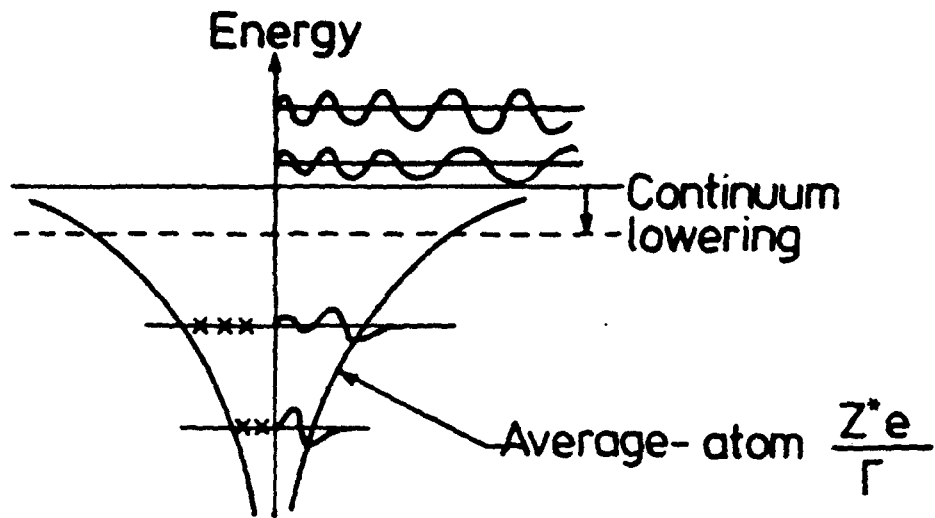
The code PPP is in good shape.

It is very fast and easy to use on work-stations. However, it has not been properly designed to join other codes.

Stochastic Stark effect is accounted for multi electron emitters in plasmas. This is particularly useful for impurity ions and for further developments.

S. ROSE
NIMP TALK

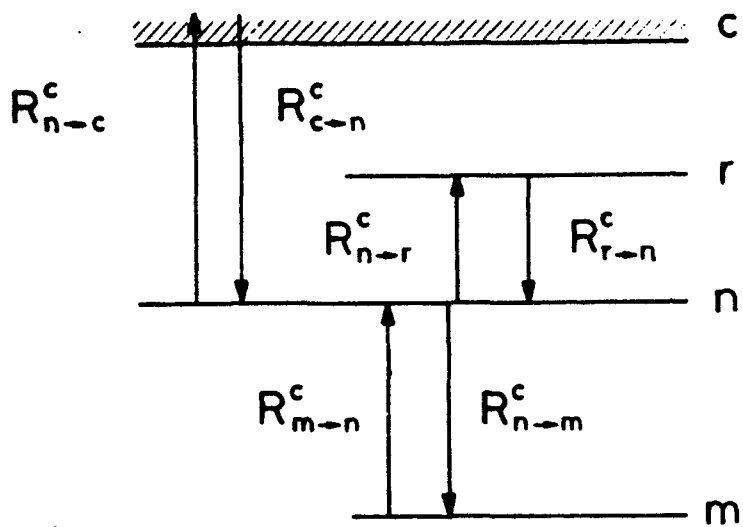
Non-LTE average-atom model



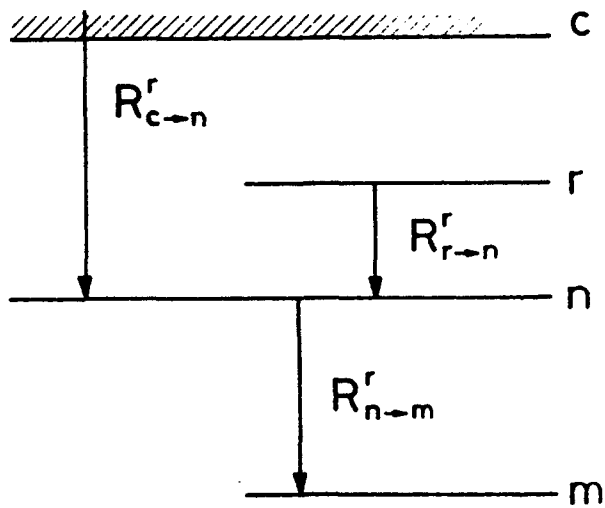
$$\left. \begin{array}{l} R_{n \rightarrow m}^C, R_{m \rightarrow n}^C \\ R_{n \rightarrow c}^C, R_{c \rightarrow n}^C \\ R_{n \rightarrow m}^r \\ R_{c \rightarrow n}^r \end{array} \right\} \begin{array}{l} \text{electron} \\ \text{collision} \\ \text{rates} \\ \\ \text{spontaneous} \\ \text{radiative} \\ \text{rates} \end{array} \right\} \begin{array}{l} \text{simple} \\ \text{scaling} \\ \text{with} \\ Z^* \end{array}$$

$$\frac{dp}{dt} = f(R)$$

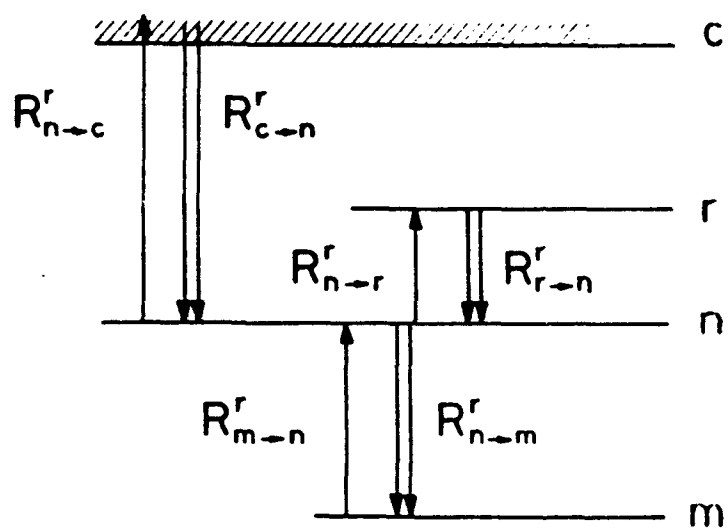
Solved for each timestep in each Lagrangian cell



collisional
rates



spontaneous
radiative
rates



stimulated and spontaneous
radiative rates

sum of radiative
and collisional rates
from shell m to n

$$\frac{dP_n}{dt} = \text{---} + P_m \left(1 - \frac{P_n}{2n_n^2} \right) (R_{m \rightarrow n}^c + R_{m \rightarrow n}^r) + \text{---}$$

number of
electrons in
shell m

probability of a
hole existing in
shell n, Q_n

$$\frac{dP_1}{dt} = f_1 (P_1, \text{---}, P_{n_{\max}}, R)$$

⋮

$$\frac{dP_{n_{\max}}}{dt} = f_{n_{\max}} (P_1, \text{---}, P_{n_{\max}}, R)$$

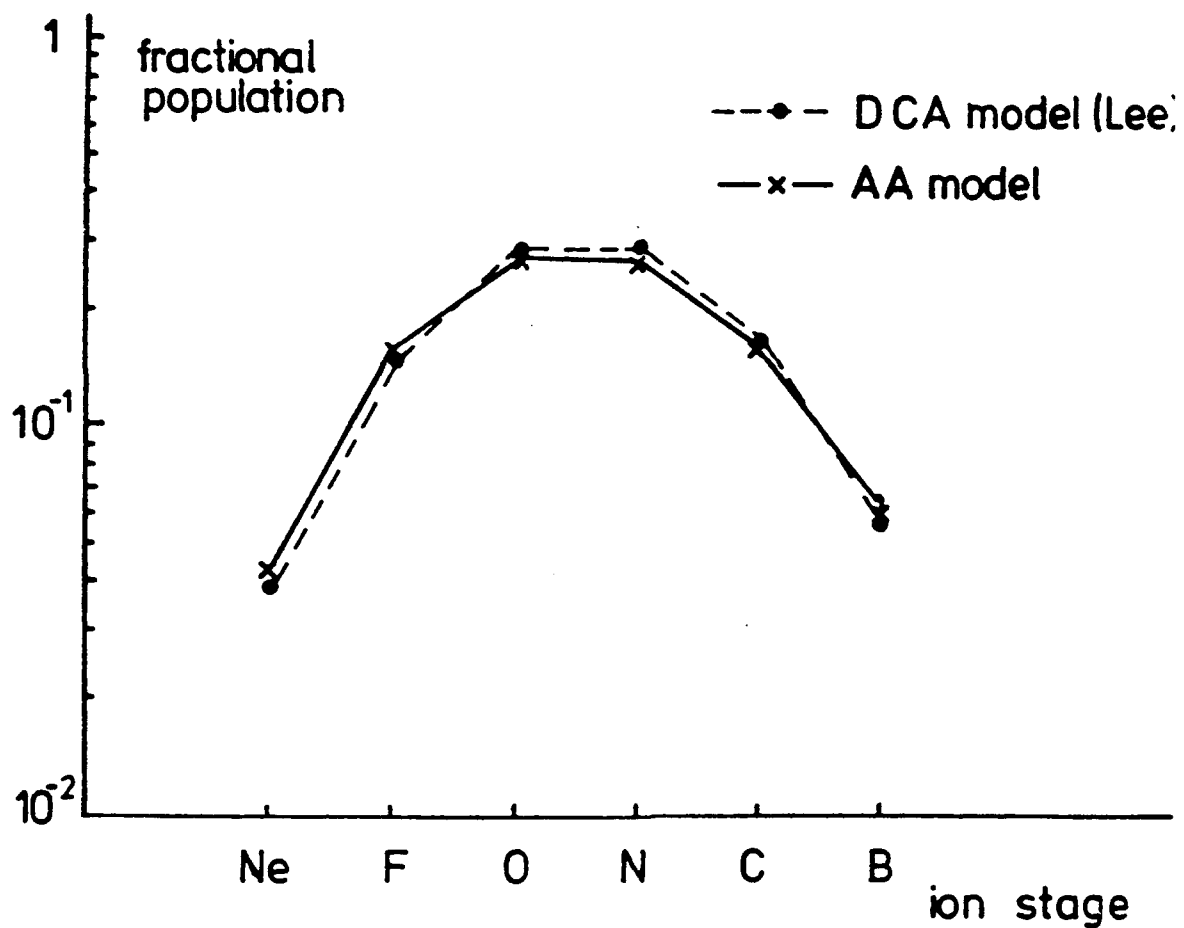
solved for
 $P_1, \text{---}, P_{n_{\max}}$
by an
iterative method

From the average populations ($P_i, \dots, P_{n_{\max}}$) the fraction of ions in a real configuration α ($n_i, \dots, n_{n_{\max}}$) can be calculated assuming the orbitals are not statistically correlated

$$P(\alpha) = \prod_i g_i (P_i / \omega_i)^{n_i} Q_i^{\omega_i - n_i}$$

$$\frac{\omega_i!}{(\omega_i - n_i)! n_i!}$$

Comparison of AA and DCA calculations of
charge-state abundance for a selenium plasma
at $n_e = 5 \times 10^{20} \text{ cm}^{-3}$ and $T_e = 1000 \text{ eV}$
(no dielectronic recombination)



Other areas in which NIMP has been used

(i) NIMP has been used for simple studies of short-pulse ionised gases which involve a mixture of tunnel ionisation and collisional effects.

(ii) NIMP is coupled to the one-dimensional hydrodynamics code MEDUSA - the energetics of excitation and ionisation are coupled self-consistently to the hydrodynamics.

Applications:

Long-pulse X-ray lasers - recombination and collisional excitation.

Short-pulse X-ray lasers - recombination (including the tunnel ionisation rates).

Emission spectroscopy - high-resolution in large velocity gradient..

Absorption spectroscopy - laser-heated and X-ray heated.

A model for line transfer in plasmas with large velocity gradients.

**A. Djaoui, S. J. Rose, (Theory),
J.S. Wark, H. He, O.Renner, T. Missalla, E. Foerster (Experiments)**

- . Description of experiment.
- . Description of model.
- . Results and comparison with experimental data.
- . Conclusions



Experiment measures Al Ly- α for various angles of observation with respect to laser beam.

- **Target:**

Al foil, 10 μm thick, 500 μm diameter.

- **Laser:**

80 J, 0.53 μm in 1.2 ns (FWHM) pulse.

Focal spot diameter 350 - 75 μm

Intensity 7×10^{13} - 1.5×10^{15} W/cm²

- **Double Crystal Spectrometer:**

Spectral resolution 6850, Dispersion on film 6.5 mÅ/mm.

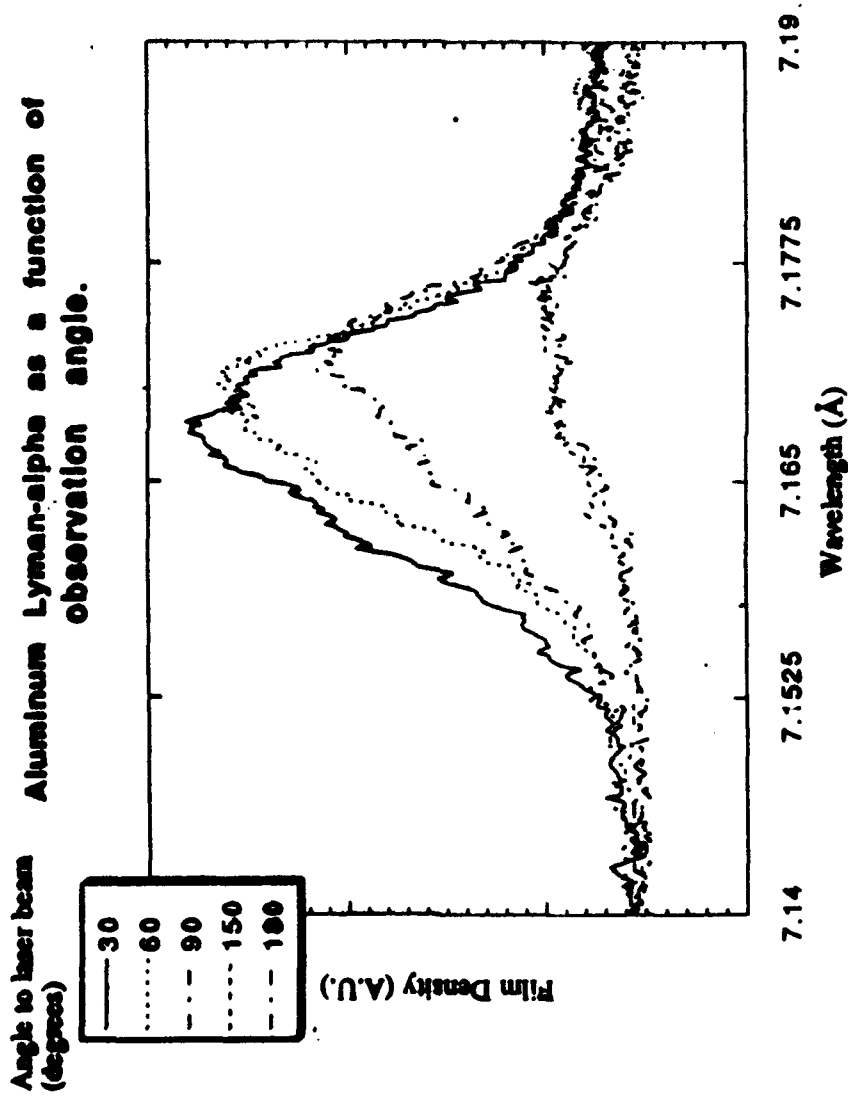
$\Delta\lambda_{\text{Dop}}(\text{Ti}=700 \text{ eV}) = 2.8 \text{ mÅ.}$

$(\Delta\lambda_{\text{Dop-shift}}(V=5 \times 10^7 \text{ cm/s}) = 12 \text{ mÅ.})$

A model for line transfer in plasmas with large velocity gradients.



Assymmetric line profiles, Emission almost independent of angle on red side of line.



A model for line transfer in plasmas with large velocity gradients.

For each timestep there are 3 coupled problems: hydrodynamics, ionic level populations and radiation transfer.

Stage 1: Hydrodynamic and level populations solved self-consistently

- 1 D lagrangian hydrodynamic code with various Equation of states.
- Time dependent average atom model includes:
 - Collisional ionization/Three body recombination
 - Collisional excitation/Collisional de-excitation
 - Radiative emission
 - Radiative recombination
- Coupling of energies of above atomic processes to free electron energy balance equation.
- Continuum radiation optically thin
- Escape factors on Lyman-series

A model for line transfer in plasmas with large velocity gradients.



Given temperatures, densities, velocities and ionic populations from stage 1

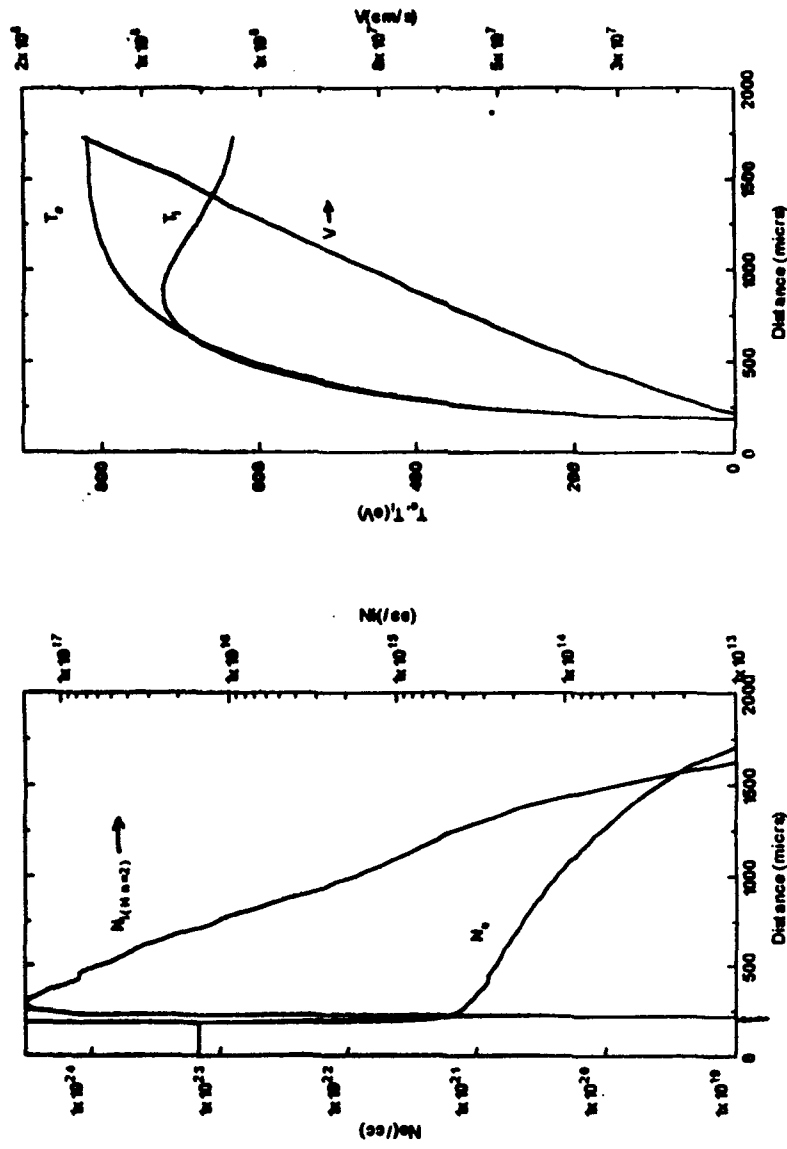
Stage 2: Detailed line transfer for Ly- α doublet in planar geometry

- . For each angle and each frequency (in lab frame), compute frequency in emitting cell frame.
- . In each lagrangian cell: emission from $1s_{1/2} - 2p_{1/2}$ (line centre at 7.181 Å) and $1s_{1/2} - 2p_{3/2}$ (line centre at 7.176 Å) added together.
- . Population of $n=2$ states ($2s_{1/2}, 2p_{1/2}, 2p_{3/2}$) according to degeneracy.
- . Effect of reabsorption on $n=2$ level (included in stage 1)
- . Absorption by both components taking into account macroscopic Doppler shifts between the emitting and absorbing cells.
- . Choice of Stark (Lee's model) or Doppler line profile

A model for line transfer in plasmas with large velocity gradients.

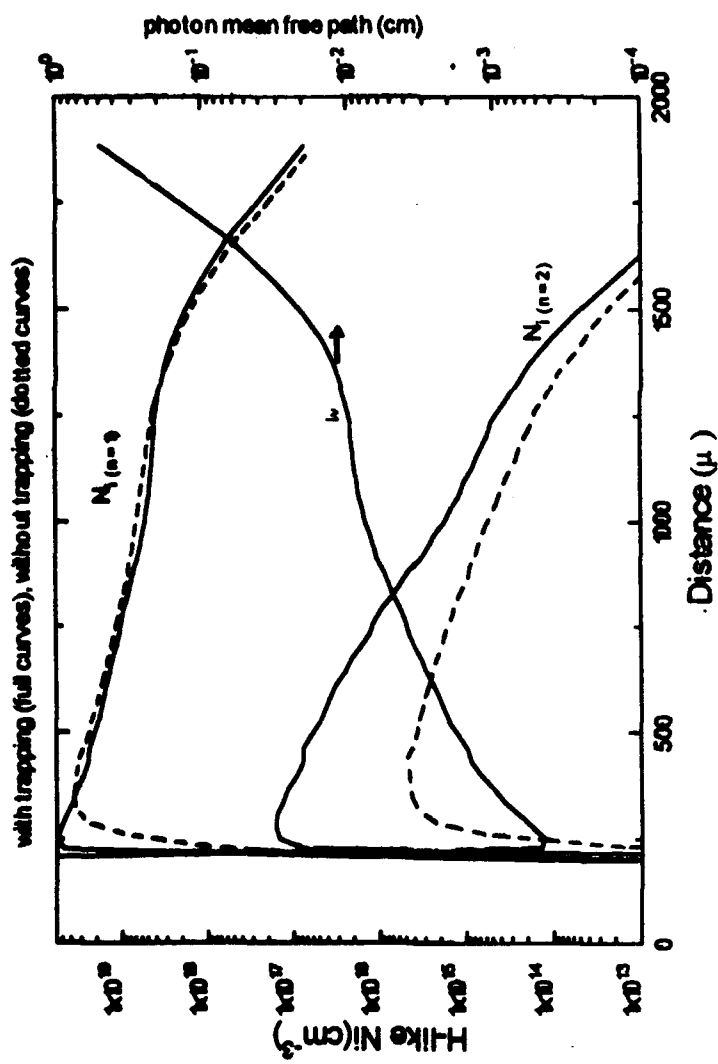


Profiles 1ns after peak of laser pulse



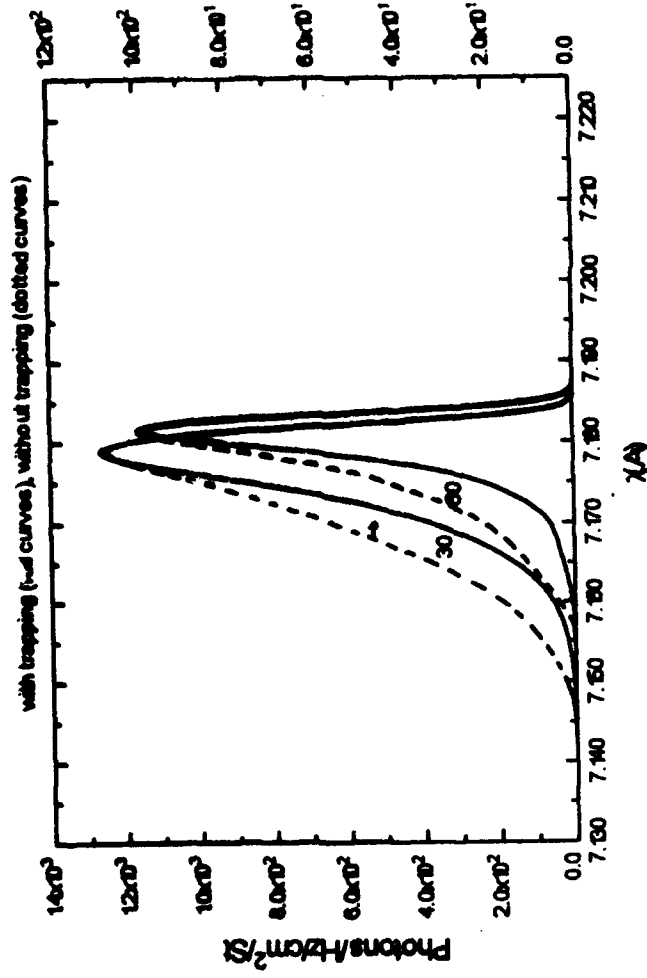
A model for line transfer in plasmas with large velocity gradients.

Effect of trapping on n=2 population



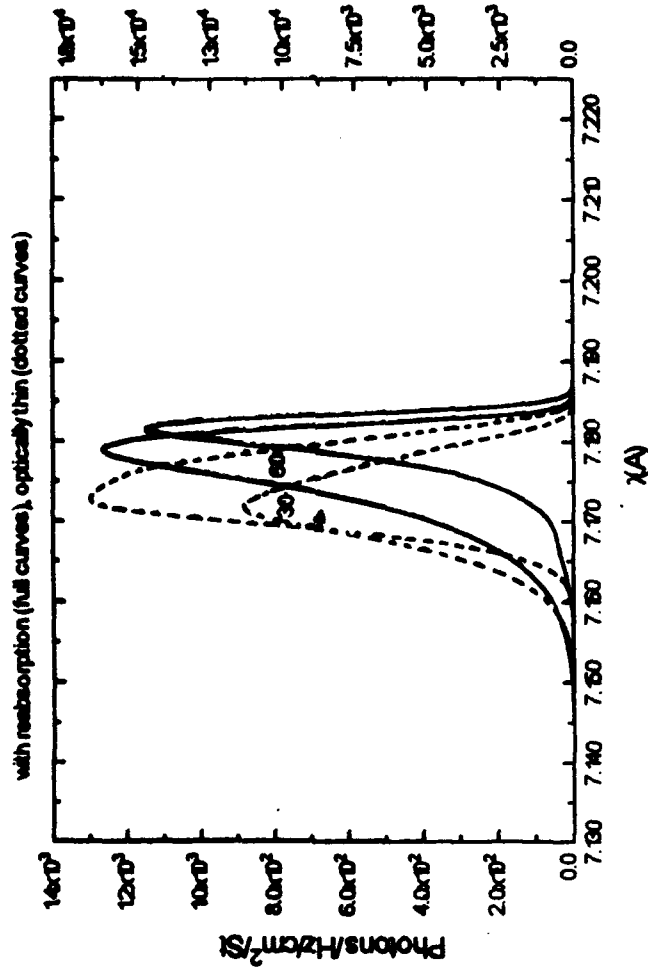
A model for line transfer in plasmas with large velocity gradients.

Trapping affects line intensity more than line shape.



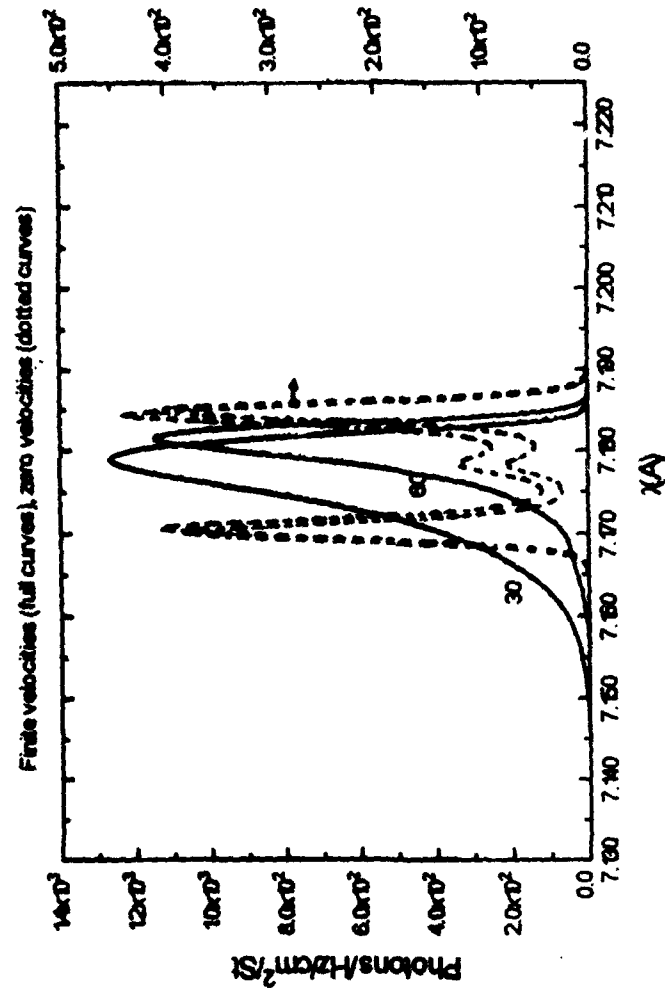
A model for line transfer in plasmas with large velocity gradients.

Transfer of radiation is important in order to account for both line shape and intensity.



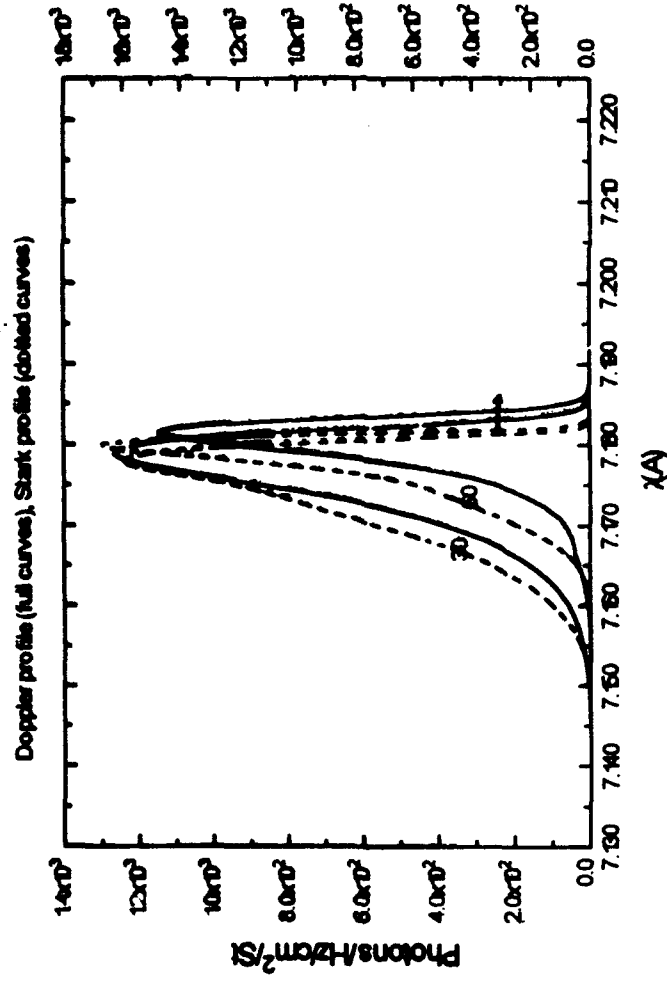
A model for line transfer in plasmas with large velocity gradients.

Spectrum from static plasma bears no resemblance to finite velocity case.



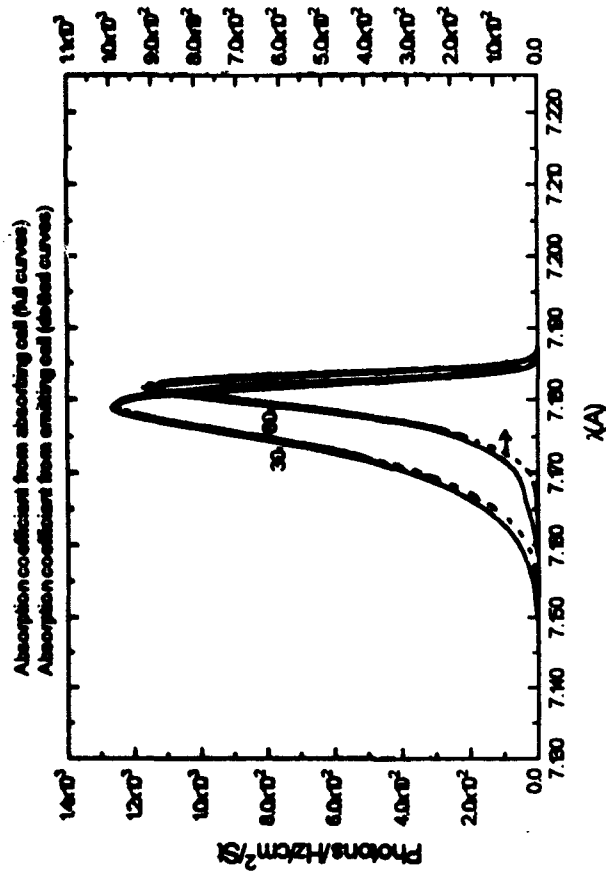
A model for line transfer in plasmas with large velocity gradients.

Stark profile not important in this case (emission from $\text{Ne} \approx 10^{21} \text{ cm}^{-3}$)



A model for line transfer in plasmas with large velocity gradients.

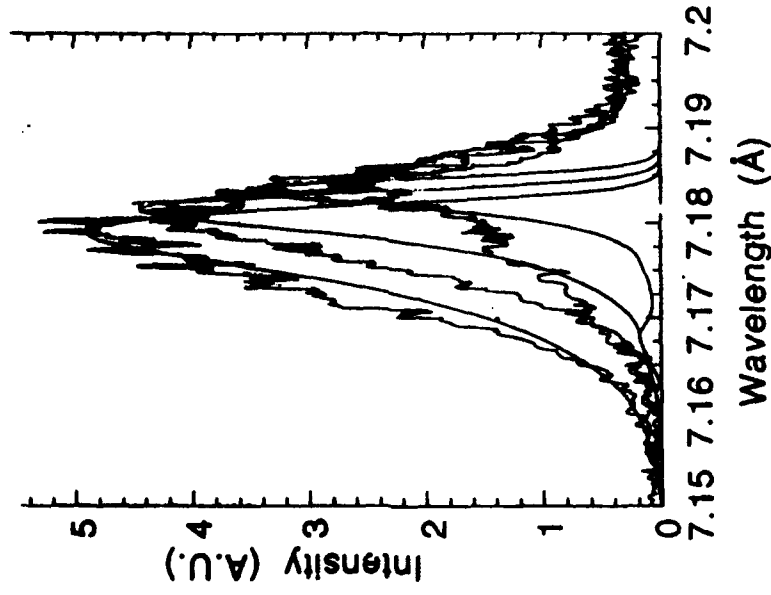
Using absorption coefficient from emission zone throughout plasma (in a similar way to escape probability method) has little effect.



A model for line transfer in plasmas with large velocity gradients.

Reasonable agreement between model and experiment for forward emission.

Slope on red side: 2 D effects and/or emission near ablation surface (Stark)



A model for line transfer in plasmas with large velocity gradients.

Conclusions

- Accurate evaluation of lineshapes should involve line transfer calculations which take into account macroscopic Doppler shift.
- In order to account for absolute experimental intensities, escape factors (or full radiation transport) should be used.
- By decoupling the effect of radiation on populations (as opposed to self consistent radiation transport and ionic population kinetics), it is possible to simulate line emission from laser produced plasmas with reasonable accuracy.

A model for line transfer in plasmas with large velocity gradients.



HYADES

**A radiation hydrodynamics code
for dense plasma studies**

**Jon T. Larsen
Cascade Applied Sciences, Inc.
Boulder, CO**

**Workshop on Models for Plasma Spectroscopy
St. John's College
Oxford, U.K.
September 27-30, 1993**

HYADES is a hydrodynamics simulation code for the experimenter*

- **Help understand and interpret lab experiments**
- **Aid in setting diagnostic instruments**
- **Easy to use input and output**
- **Choice of physics models**
- **Simple approximations to physics models**
- **Runs on a variety of computers: PCs and Macs
to Crays**

* Theorists are permitted to use it too!

HYADES has many features that makes it a powerful numerical simulation tool



One dimensional; three geometries	Multigroup radiation transport
Several ionization models	In-line, tabular cold, and external tabular opacities
Lagrangian hydrodynamics tabular and ideal gas EOS materials strength fracture models	LTE and nonLTE atomic physics
Separate electron, ion, radiation temperatures	Thermonuclear burn
Flux-limited electron and ion diffusion; nonlinear and thermal conductivities	Multiple laser deposition
	Extensive energy source options and flexible specifications
	Restart capability
	Flexible post-processing capability

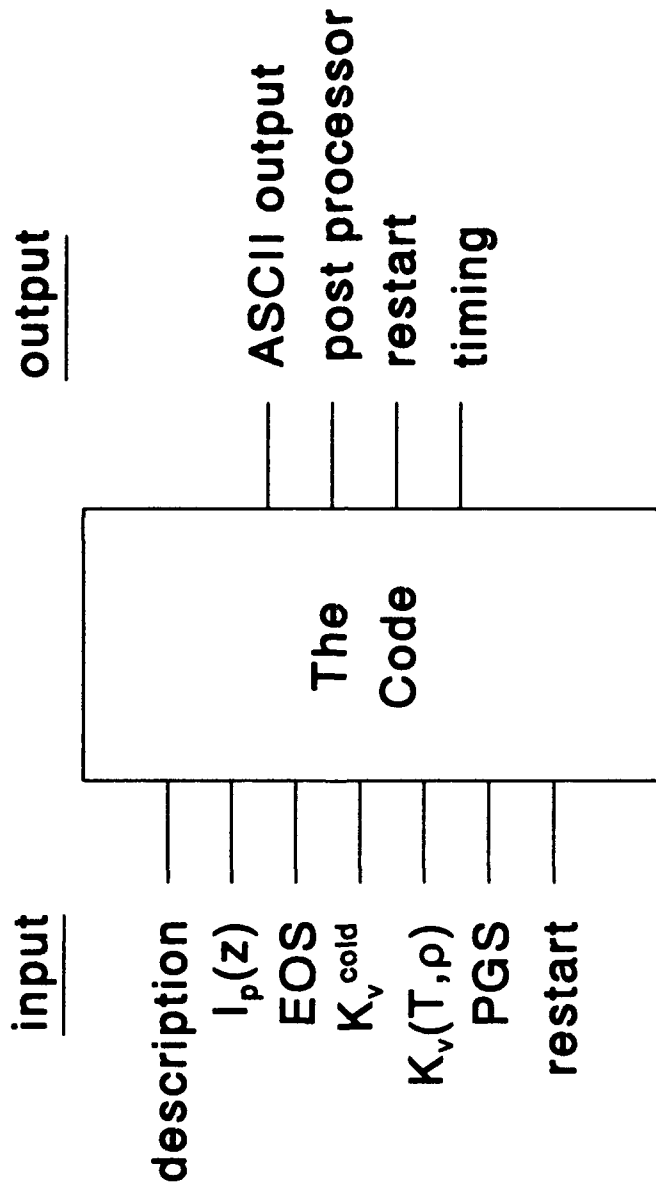
A design "philosophy" for HYADES



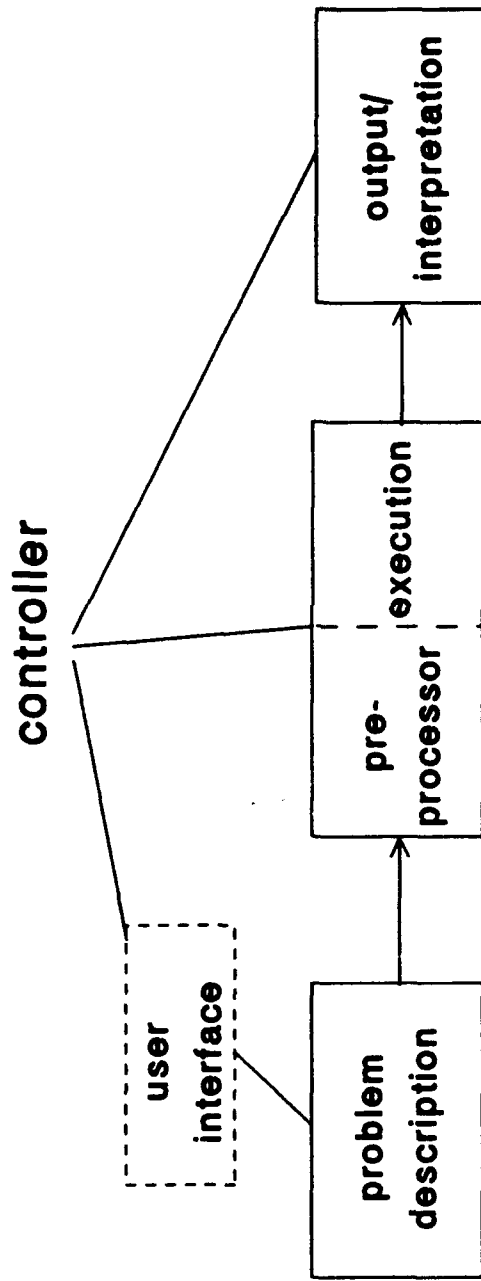
- 1. Flexibility**
 - basic set of default models**
 - user can modify models via parameters or**
 - select more accurate models**
- 2. Put in physics that affects "bulk" properties -**
 - "simple" approximations**
- 3. Minimize user created errors**
- 4. Runs in a reasonable amount of time**

00-092493-03

HYADES uses a variety of external files



HYADES will integrate easily into ADAM



00-092493-05

Conservation of momentum is solved by a time-explicit algorithm

- Lagrangean prescription
- Newton's second law

$$\rho \frac{\partial u}{\partial t} = - \nabla (P + Q)$$

$$P = P_o + P_i + P_r$$

Q has both real and artificial viscosities

- Pressures obtained from realistic EOS tables or ideal gas model

**At high velocities pressure waves may
steepen to form shock fronts**

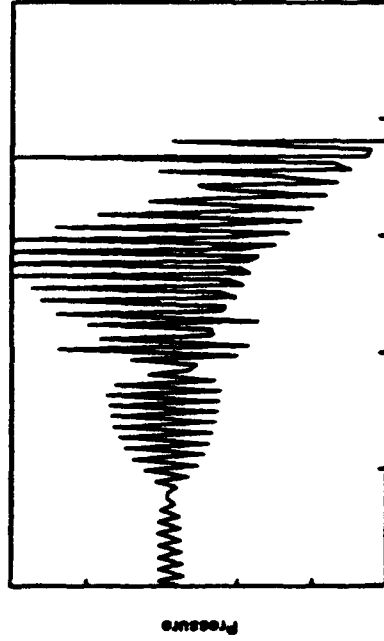


**Viscous effects convert kinetic energy
into thermal energy**

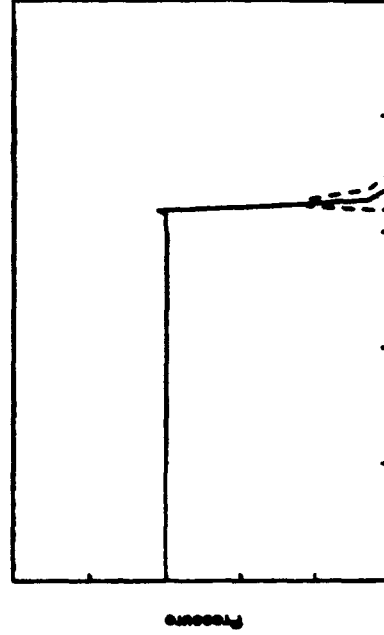
Add an artificial viscous stress to the pressure

$$Q = -\rho (\Delta x)^2 (\partial v / \partial x)^2$$

without Q



with Q



00-101293-01

Position

Position

Thermal energy is transported by several mechanisms



$$\rho C_v \frac{\partial T_1}{\partial t} = -P_d V \cdot \nabla \cdot Q - W_{12}(T_1 - T_2) + \dot{S}$$

- Thermodynamic coefficients from EOS tables or ideal gas model
- Nonlinear thermal conductivities limited by free-streaming flux

$$Q = -K_{\text{eff}}(T) \nabla T \quad K_{\text{eff}} = \frac{K_e^{\text{sh}}}{1 + \frac{K_e^{\text{sh}}}{K_e^{\text{fs}}}}$$

- Ions are treated classically
- Electrons are nonrelativistic but degeneracy effects are included

Classical electron conductivity model fails in steep temperature gradients



- At the laser ablation front

$$\lambda_e \approx v_e T_d \approx 1.4 \times 10^{10} \frac{T_e^2}{n_i Z^4 \ln \Lambda_{ei}} > T_e \frac{dx}{dT_e}$$

- Use harmonic mean between free-streaming and modified Spitzer-Harm conductivities

$$K_e^{sh} \sim \frac{T_e^{5/2}}{Z^2 n_e \ln \Lambda_{ei}} \quad K_e^{sh} = f \frac{n_e m_e v_e^3}{|VT_e|}$$

- Flux limiter is ad hoc but motivation is physical and gives approximate correct behavior.

An improved thermal conduction model works at "room" temperature



Using the Coulomb cross section in the Boltzmann equation gives

$$K_0 = \frac{n_0 k (kT_0)}{m_0} \tau_0 A^p(\mu/kT_0)$$

Average electron relaxation time is

$$\tau_0 = \frac{3 m_0^{1/2} (kT_0)^{3/2}}{2(2\pi)^{1/2} Z^2 n_i e^4 \ln \Lambda_{ei}} [1 + \exp(-\mu/kT_0)] F_{1/2}$$

In the classical limit, one gets Spitzer's value

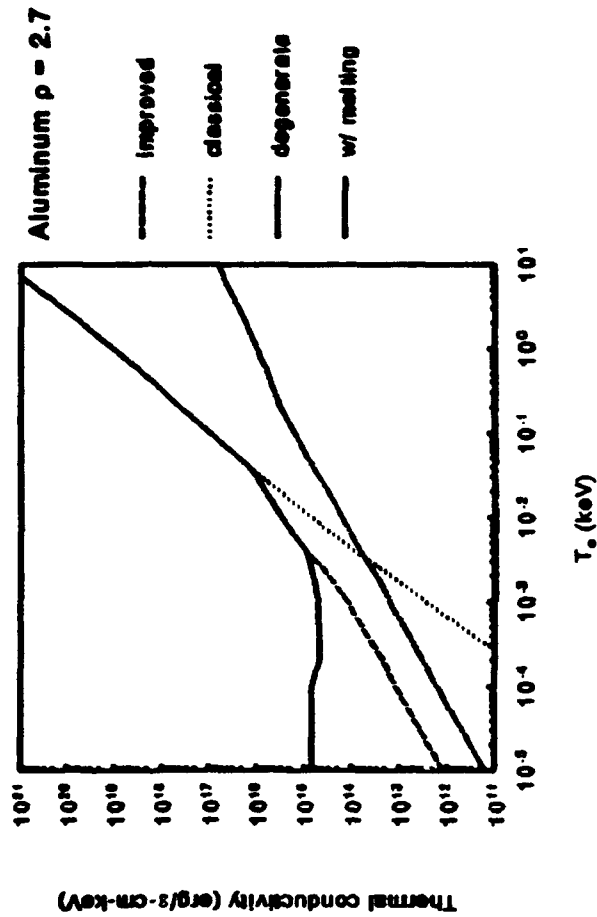
$$K_0^{sh} = \frac{128}{3\pi} \frac{n_0 k (kT_0)}{m_0} \frac{3}{4} \left(\frac{m_0}{2\pi} \right)^{1/2} \frac{(kT_0)^{3/2}}{Z^2 n_i e^4 \ln \Lambda_{ei}}$$

An improved thermal conduction model (continued)



And in the degenerate limit

$$K_d = \frac{\pi^2}{3} \frac{n_e k (kT_e)}{m_e} \frac{3}{32\pi^2 m_e Z^4 e^4 \ln \Lambda_{ei}} \frac{h^3}{3}$$



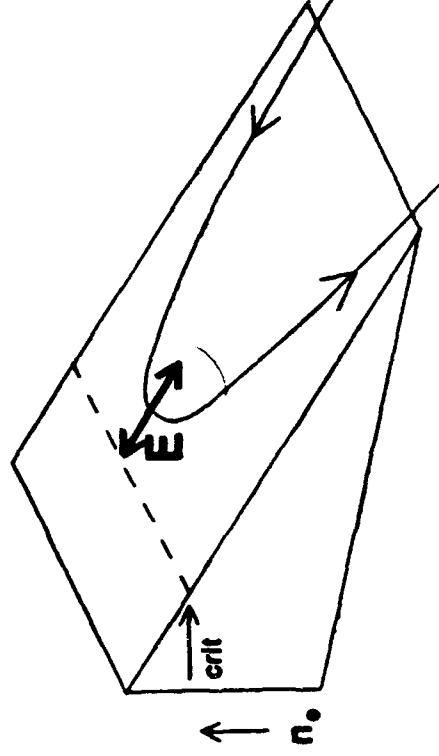
00-072893-03

Laser light is absorbed by electrons

- Frictional (3-body) processes -
inverse bremsstrahlung

$$K \sim \frac{Z^2 n_e n_i \ln \Lambda_e}{T_e^{3/2} \omega^2 \epsilon^{1/2}}$$

- Electron plasma and ion acoustic waves
- Parametric and resonant processes



00-100993-05



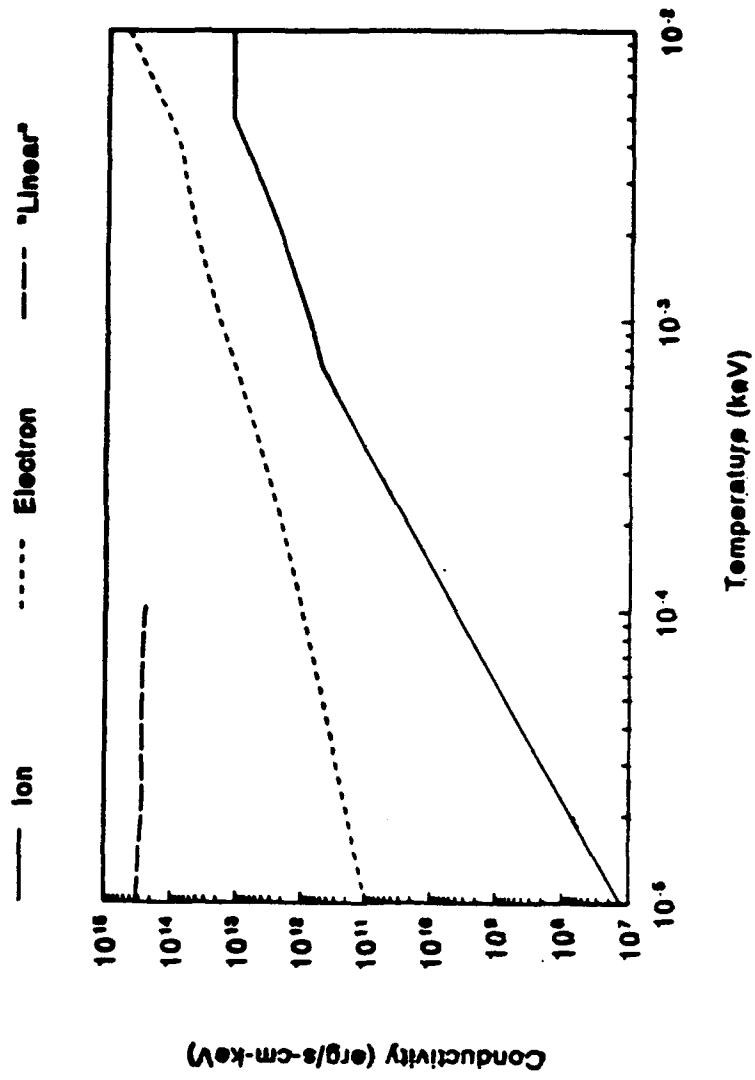
Center for
Applied
Sciences

New features and improvements have extended the capabilities

- Improved average-atom LTE model
- Cold opacities and external opacity tables
- More source types allowed including frequency-dependent radiation
- Linear heat conduction for sub-eV temperatures
- Strength of materials and fracture models
- Planar to spherical flow

Linear thermal conductivity is used for low temperatures

Aluminum $\rho = 2.7 \text{ gm/cm}^3$



Low temperature materials require strength and fracture models

The momentum equation now written with a stress tensor

$$\rho \frac{\partial \mathbf{u}}{\partial t} = \mathbf{f} + \nabla \cdot \mathbf{T}$$

$$\mathbf{T} = -P\mathbf{I} + \boldsymbol{\sigma}$$

The viscous stress tensor is

$$\sigma_{ij} = \mu \left(\frac{\partial u_i}{\partial x_j} + \frac{\partial u_j}{\partial x_i} \right) + \left(\zeta - \frac{2}{3} \mu \right) \nabla \cdot \mathbf{v}$$

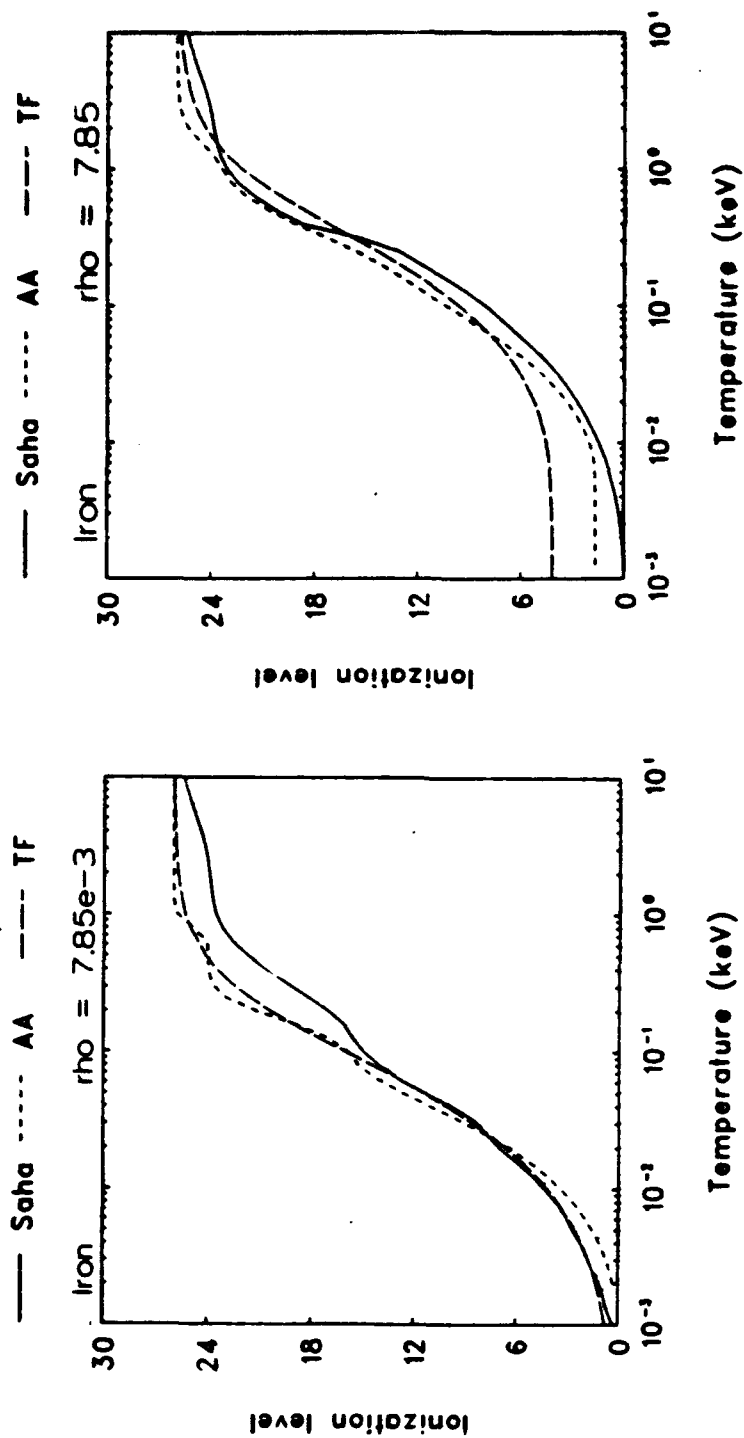
Elastic stress deviators are related to the strains

$$\sigma_{ij} = 2\mu \left(E_{ij} - \frac{1}{3} \frac{\Delta V}{V} \delta_{ij} \right)$$

A material yields when

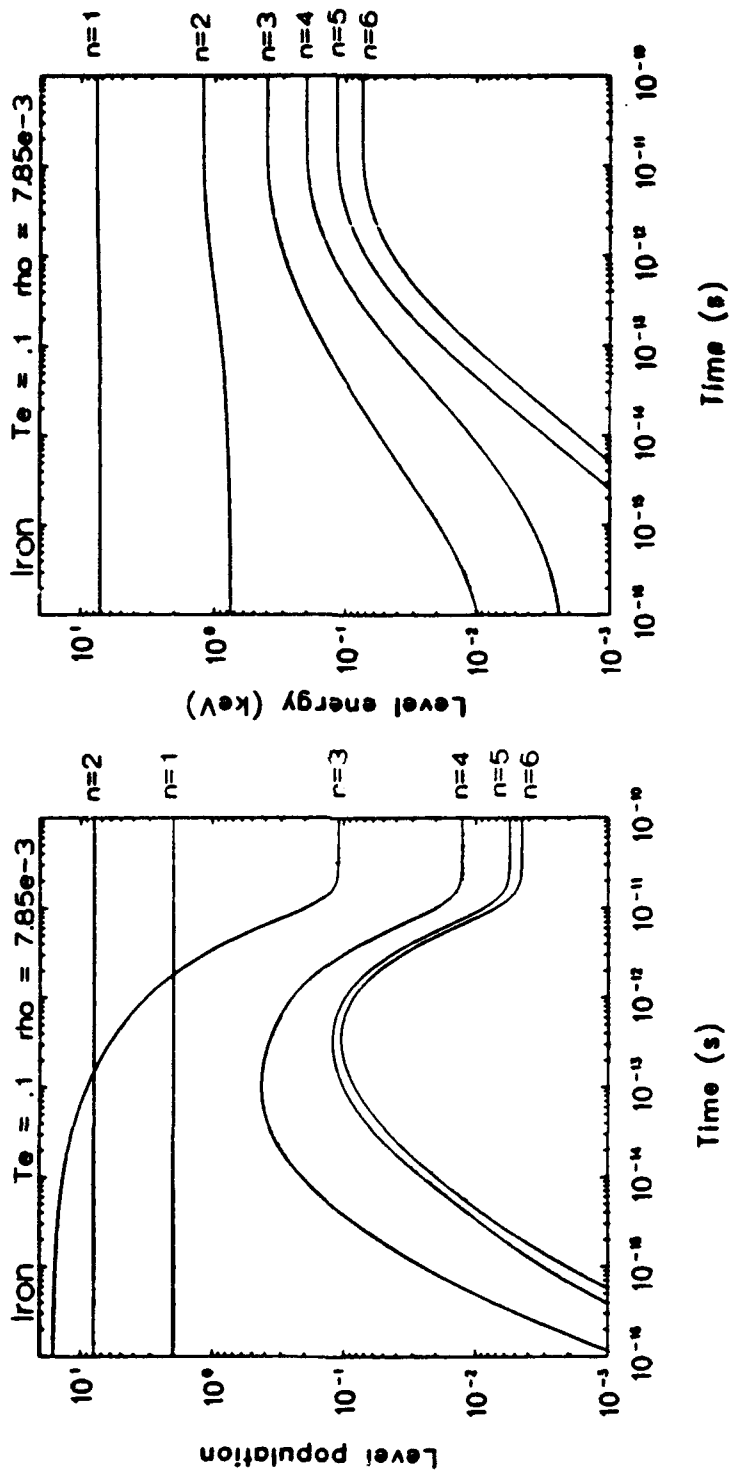
$$\Sigma \sigma^2 \geq \frac{2}{3} Y^2$$

Three ionization models give different values



101190-01

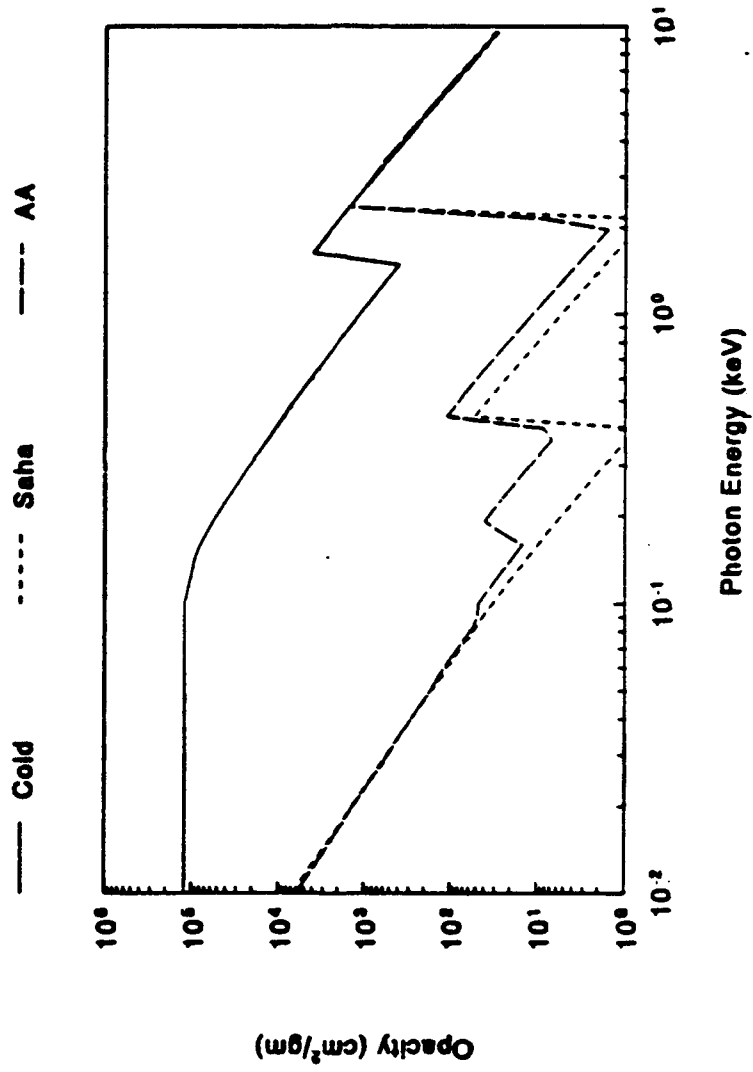
Integration of the rate equations gives the time-dependent populations and energies



00-101190-02

HYADES ionization models yield different opacities

Aluminum $\rho = 2.7 \times 10^{-3} \text{ gm/cm}^3$ $T_e = .1 \text{ keV}$



00-102592-03

A simple first example



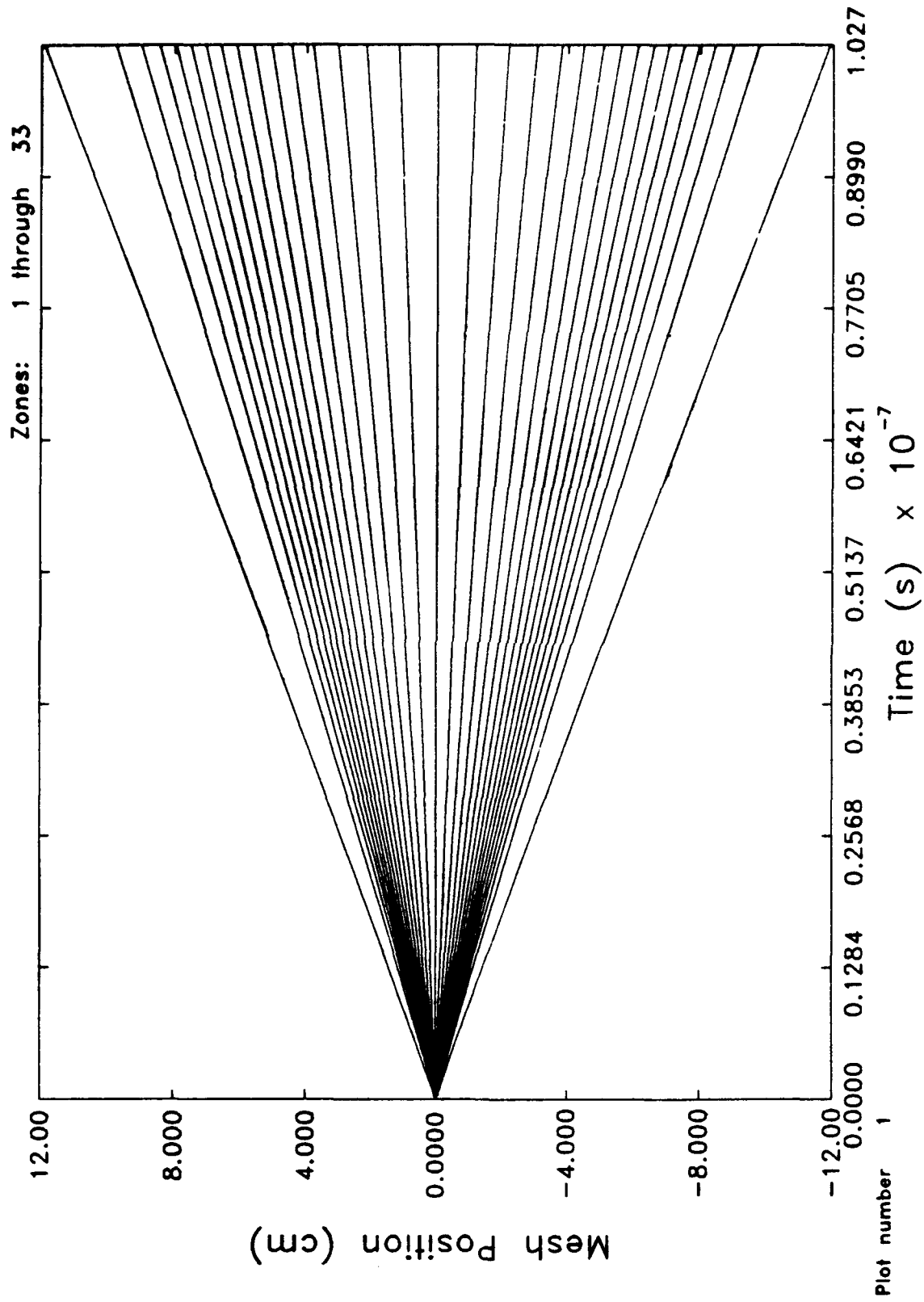
Static aluminum block

```
c
c 50µm Al slab; feathered both sides
c
mesh 1 17 -.0025 0. 1.25
mesh 17 33 0. .0025 .8
region 1 32 1 2.7 1. 1. 0.
material 1 13. 26.97 1.
eos 41 1
c
pparray r rcm deni dene zbar pres te ti u
parm postdt 1.e-9
c
parm dtmax 1.e-8
parm editdt 1.e-8
parm tstop 1.e-7
```

00-092493-01

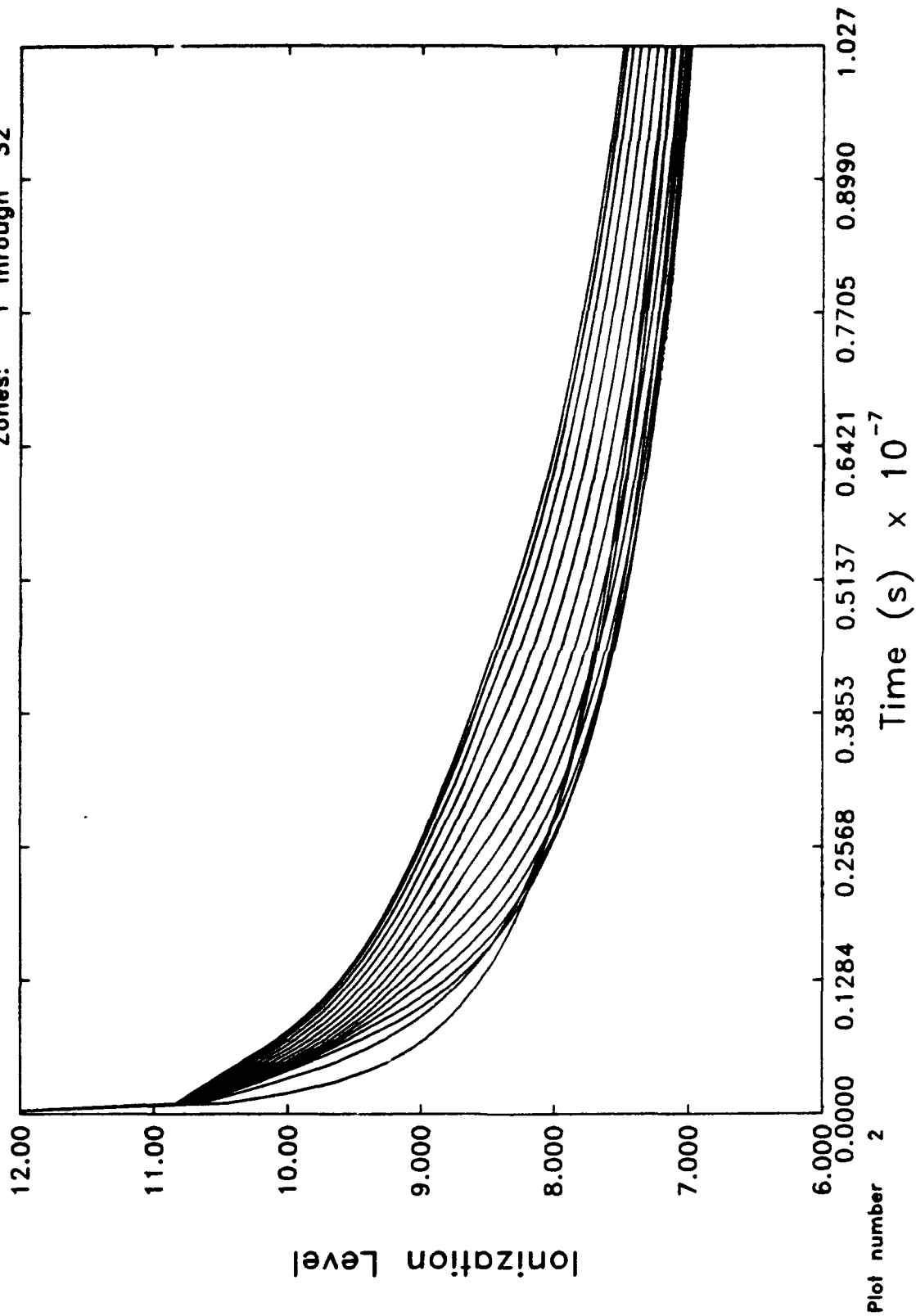
HYADES PLOT Static aluminum block
Run date: 09/24/93 09:51:14 01.05.06
Plot date: 09/24/93 10:09:42

\\hyades\examples\ex1.pst



\\hyades\examples\ex1.pst

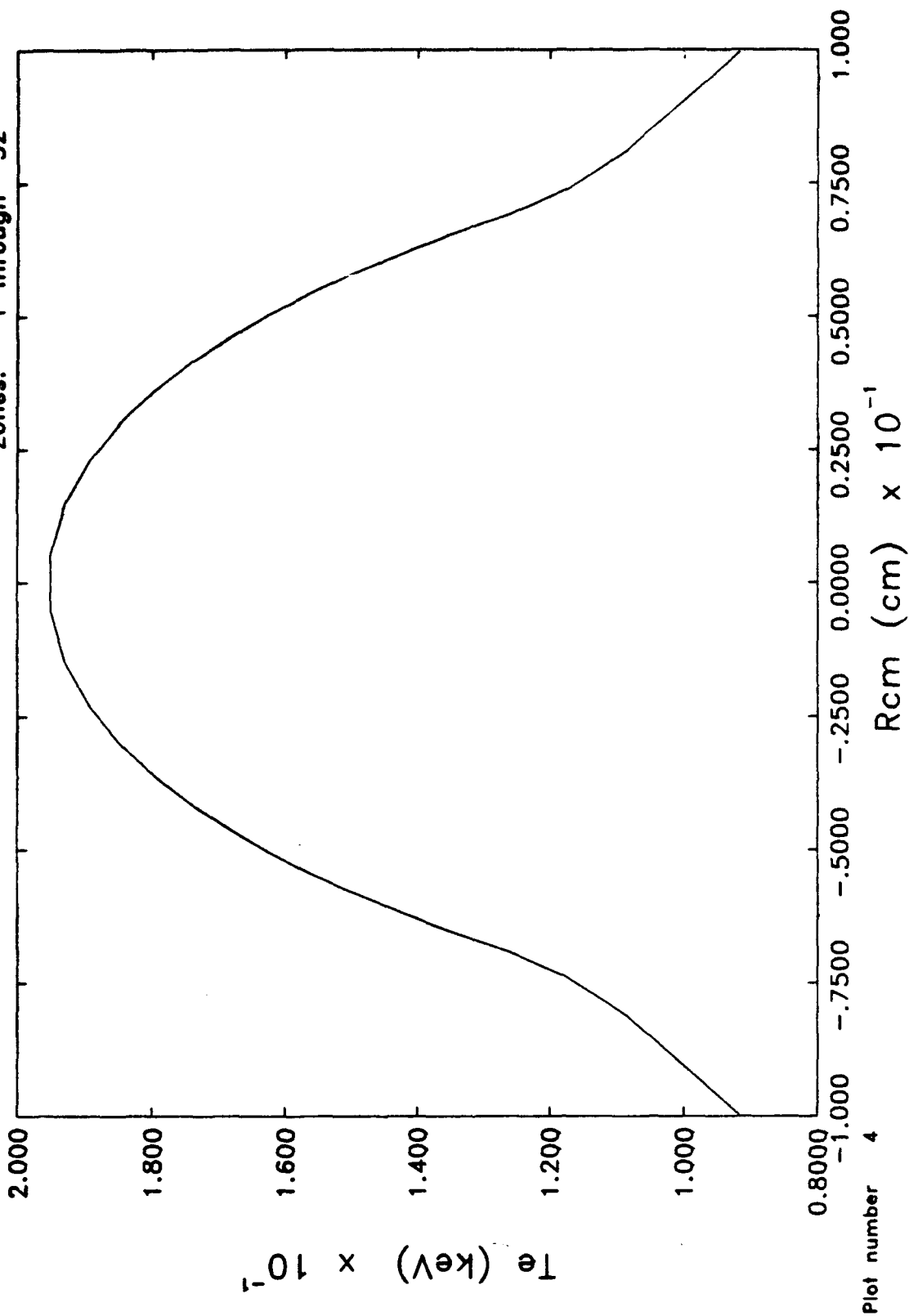
Zones: 1 through 32



HYADES PLOT Static aluminum block
Run date: 09/24/93 09:51:14 01.05.06
Plot date: 09/24/93 10:22:26

\\hyades\examples\ex1.pst

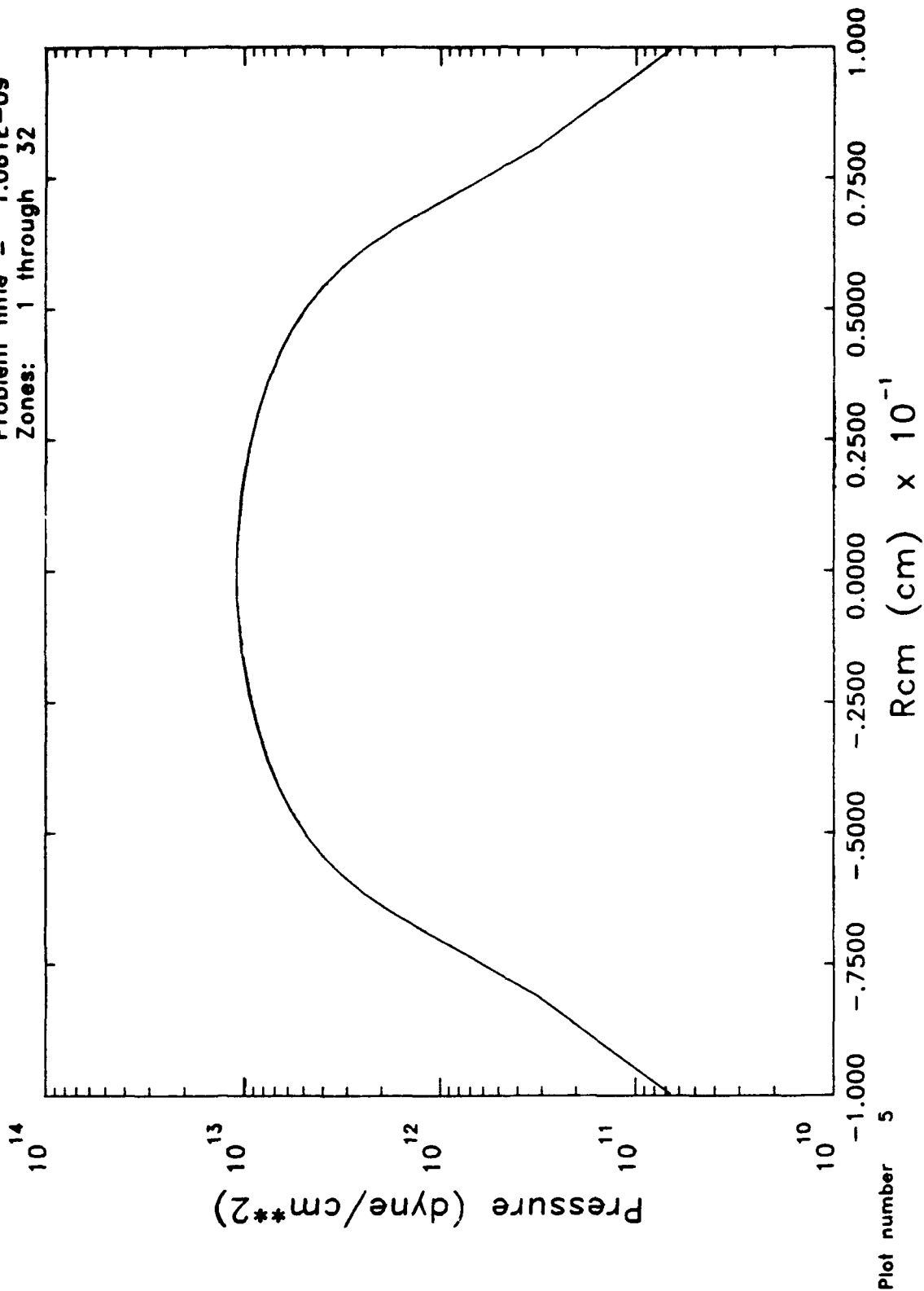
Problem time = 1.061E-09
Zones: 1 through 32



HYADES PLOT Static aluminum block
Run date: 09/24/93 09:51:14 01.05.06
Plot date: 09/24/93 10:22:26

\\hyades\examples\ex1.pst

Problem time = 1.061E-09
Zones: 1 through 32



A second example

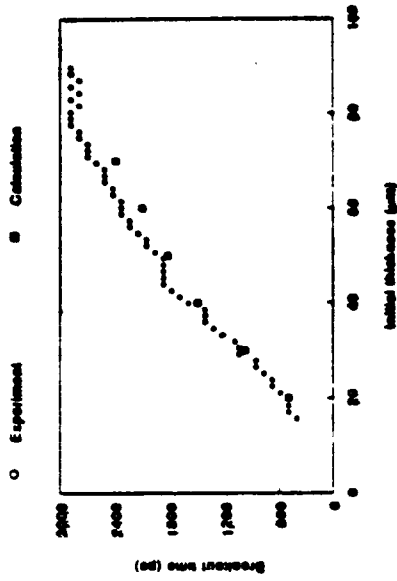
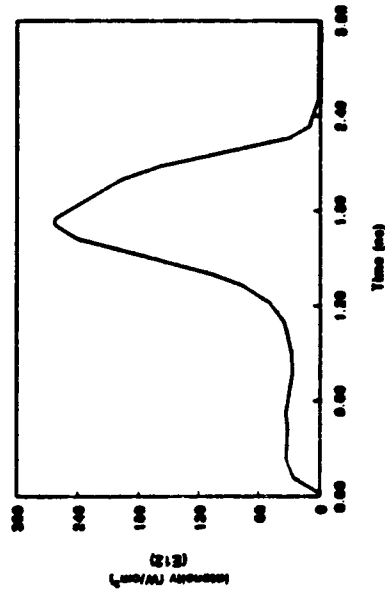
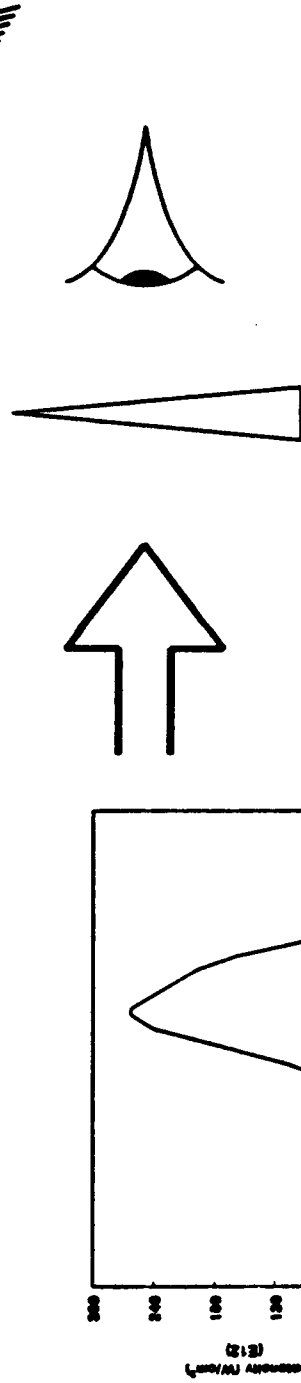
Laser accelerated aluminum slab

```
c
c 98μm Al foil, feathered on laser side
c
mesh 1 11 0. .001 1.23
mesh 11 33 .001 .0098
...
c
c 0.5μm laser on left side; 2.e14 W/cm**2
c
laser 0.53 +1
tv 0. 0.
tv 1.e-10 2.e+21
tv 2.4e-9 2.e+21
tv 2.5e-9 0.
c
```

00-092493-02

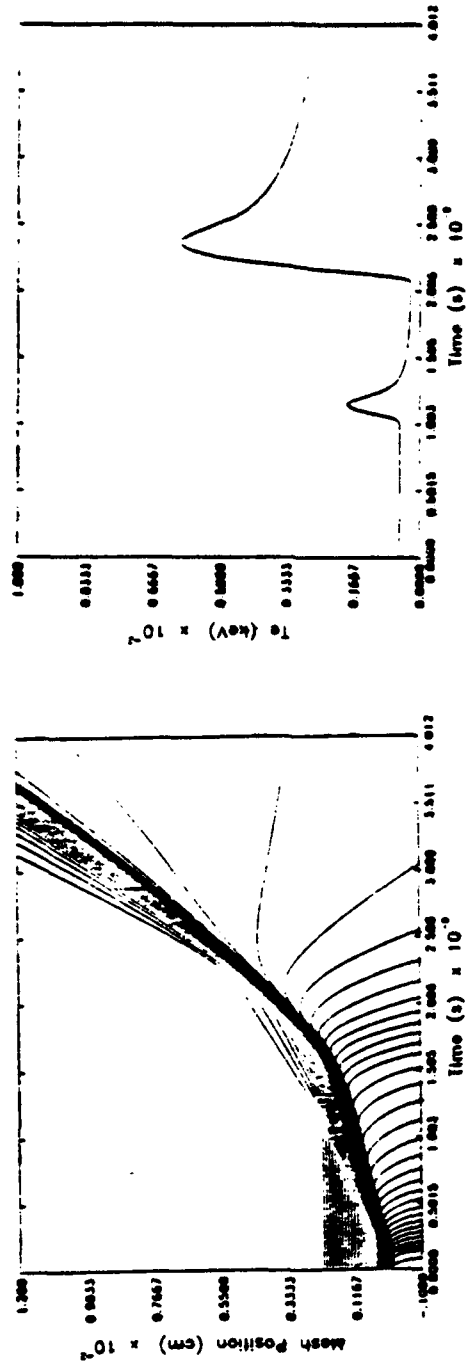


Simulation of a shock propagation experiment reproduces "breakout" times



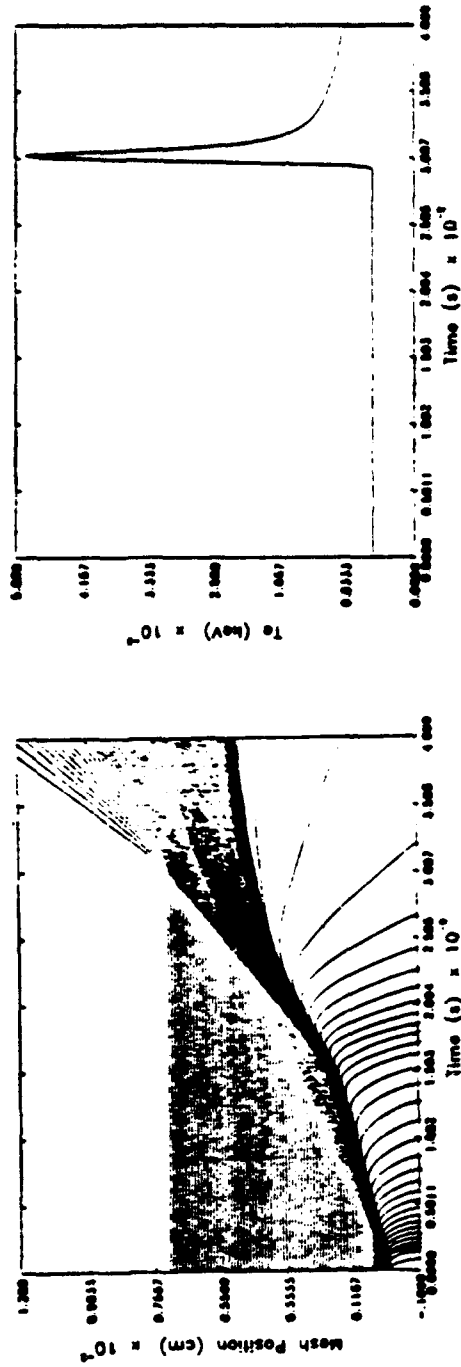
00-102692-01

Two shocks are observed for thin samples



00-102792-01

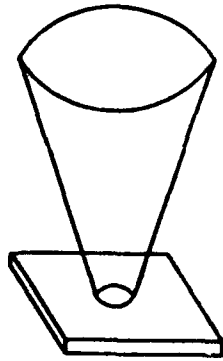
The strong shock catches the first shock in thick samples



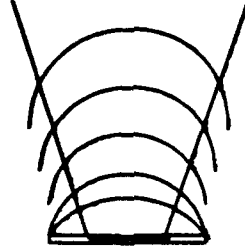
00-102792-02

Simulation of a laboratory experiment shows the effects of a divergent expansion

Al microdot target



Laser: $\lambda = .526 \mu\text{m}$
 $I = 5 \times 10^{12} \text{ W/cm}^2$
 $\tau = 500 \text{ ps}$

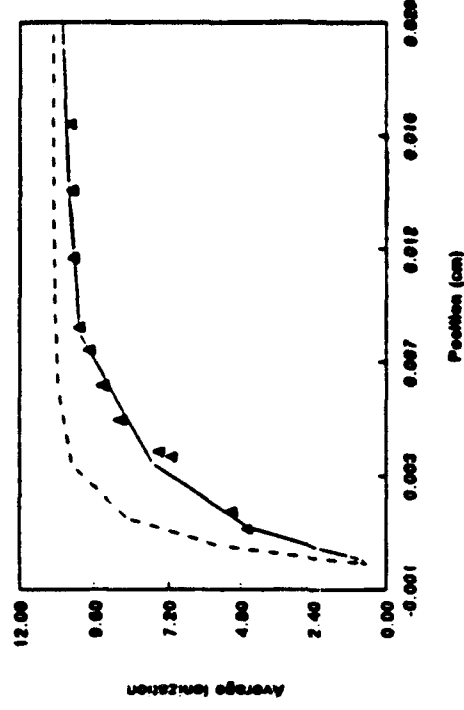
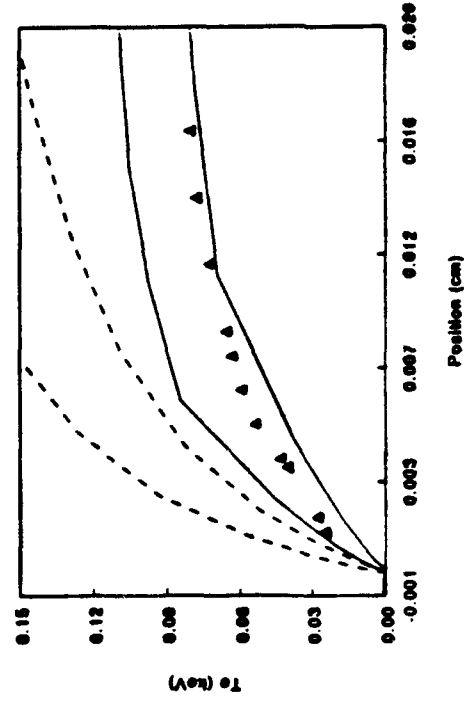


Early expansion is "planar" but develops into
a quasi-spherical flow.

Ref: C. A. Back, *et al.*, Phys. Rev. A 46, 3405 (1992).

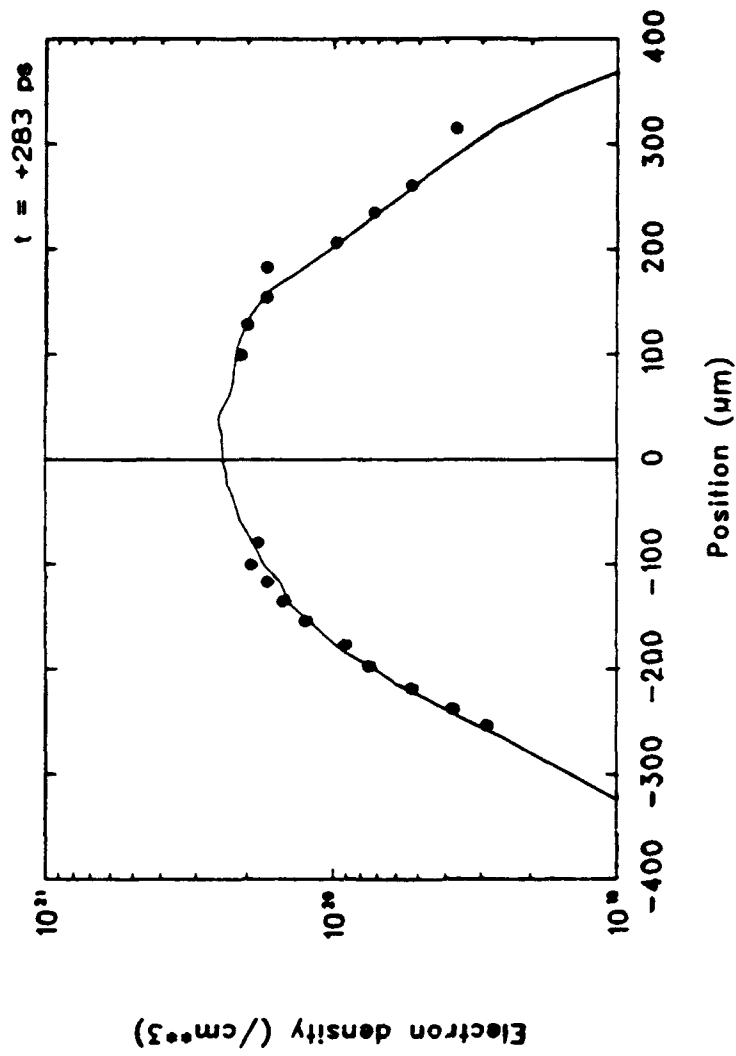
Plasma temperature and ionization level were determined by spectroscopic methods

$t \approx +1.4 \text{ ns}$



HYADES simulations show agreement if
spherical divergence is included.

HYADES reproduces the density profile of an exploding-foil target



00-101690-01



**HYADES' future directions will focus on
high laser intensities and colder materials**

- Tunnel ionization, Keldish model
- Nonlocal thermal transport
- X-ray lines in nonLTE and opacity models
- Additional radiation transport models
- More complex fracture mechanics models
- Provide an operating shell
- Develop more post-processors